Hindawi
Journal of Advanced Transportation
Volume 2020, Article ID 8842730, 21 pages
https://doi.org/10.1155/2020/8842730

WILEY | Hindawi

Research Article

Fleet Management for HDVs and CAVs on Highway in Dense Fog Environment

Bowen Gong,[1] Ruixin Wei,[1] Dayong Wu,[2] and Ciyun Lin [1,3]

[1]*Department of Traffic Information and Control Engineering, Jilin University, Changchun 130022, China*
[2]*Texas A&M Transportation Institute, Texas A&M University, College Station, TX 77843, USA*
[3]*Jilin Engineering Research Center for ITS, Changchun 130022, China*

Correspondence should be addressed to Ciyun Lin; linciyun@jlu.edu.cn

Received 22 May 2020; Revised 5 July 2020; Accepted 29 July 2020; Published 14 August 2020

Academic Editor: Chunjiao Dong

Adverse weather conditions have a significant impairment on the safety, mobility, and efficiency of highway networks. Dense fog is considered the most dangerous within the adverse weather conditions. As to improve the traffic flow throughput and driving safety in dense fog weather condition on highway, this paper uses a mathematical modeling method to study and control the fleet mixed with human-driven vehicles (HDVs) and connected automatic vehicles (CAVs) in dense fog environment on highway based on distributed model predictive control algorithm (DMPC), along with considering the car-following behavior of HDVs driver based on cellular automatic (CA) model. It aims to provide a feasible solution for controlling the mixed flow of HDVs and CAVs more safely, accurately, and stably and then potentially to improve the mobility and efficiency of highway networks in adverse weather conditions, especially in dense fog environment. This paper explores the modeling framework of the fleet management for HDVs and CAVs, including the state space model of CAVs, the car-following model of HDVs, distributed model predictive control for the fleet, and the fleet stability analysis. The state space model is proposed to identify the status of the feet in the global state. The car-following model is proposed to simulate the driver behavior in the fleet in local. The DMPC-based model is proposed to optimize rolling of the fleet. Finally, this paper used the Lyapunov stability principle to analyze and prove the stability of the fleet in dense fog environment. Finally, numerical experiments were performed in MATLAB to verify the effectiveness of the proposed model. The results showed that the proposed fleet control model has the ability of local asymptotic stability and global nonstrict string stability.

1. Introduction

Adverse weather conditions have a significant impact on the safety, mobility, and efficiency of highway networks [1]. Based on the statistical data, weather contributed to about 20% of traffic accidents, 38.3% of traffic congestion, 23% of all nonreoccurring delays and caused billions dollars' loss by closed highways, vehicle delays, and traffic accidents [2]. The consequent adverse impact on the safety and mobility of highway networks makes it important to research and develop new and more efficient methods to address highway management and operation problems during adverse weather conditions [3]. Xu [4] explored crashes under different weather conditions on the highway and found that adverse weather conditions can lead to dangerous driving conditions and greatly increase the crash rate. Moreover, due to its limited visibility and accident susceptibility, dense fog is considered the most dangerous within the adverse weather conditions [4].

Besides visibility impairments in foggy weather conditions, the ability of risk perception is reduced as the driver inability to judge the driving state and safe distance accurately. Therefore, the driver tends to continue driving until the following distance is equal to or less than the safety distance. After realizing the crash-prone traffic condition, the driver will operate the vehicle with sequential rushed acceleration or nasty deceleration to keep out of traffic accidents [5]. Furthermore, the researchers found that most drivers prefer to drive at high speeds when they cannot see the vehicle in front. In this case, even if the driver finds the vehicle in front of the visibility boundary and braking timely, it is difficult to avoid a crash [4, 6].

In addition, the dense fog weather condition will greatly reduce the driver's ability of identification traffic conditions. For example, when the visibility is less than 50 m, the driver's visual search focus will increase by 23.6%, and the scope and efficiency visual selective attention will decrease [7]. In these situations, the combination of speed perception, speed feedback, driving performance feedback, and other capabilities that support the driver to make vehicle operation decisions is not always in the best safety interest [6]. Furthermore, the individual differences among drivers must also be considered in the driving conditions, such as differences in age, gender, and psychological quality.

The internal and external adverse impact on driver behavior in dense fog environment makes it becoming the most dangerous type within adverse weather conditions [8]. Wang [9] analyzed 1,513,792 traffic accidents and found that the number of fatal traffic accidents caused by dense fog is 35 times that of clear weather. Traffic safety concerns in dense fog on the highway were intense due to the fatal traffic accidents, as the individuals and groups are increasingly concerned with the adverse weather condition impact on highway travelling [10–12].

Based on the state-of-the-art in literatures and researches for driving safely in dense fog weather conditions, the proposed methods can be divided into macrolevel and microlevel. In respect of macrolevel mode, it mainly focuses on risk prediction under dense fog weather conditions based on historical data and then makes up corresponding risk management and control approaches such as setting warning flags and installing security infrastructure. Wu [13] analyzed the effects of real-time warning systems on driving under fog conditions by comparing the effectiveness of beacons and dynamic message signs in foggy areas. Zhai [14] used the historical traffic collision data, traffic flow data, and dense fog conditions to set up a collision risk prediction model to predict the collision risk under specific visibility. Ahmed [8] predicted the risk of traffic accidents on highways near the airport in dense fog weather conditions based on variables such as airport weather data, historical crash data, and road characteristics. Hassan [15] used detectors and radar sensors to receive real-time traffic flow data, which are used to predict the likelihood of traffic accidents in low-visibility situations, and then conduct proper traffic management 5–15 minutes before the highway may collide. In this study, the probability of correctly identifying a collision reached 69%. Winkle [16] proposed a systematic safety analysis framework that combines the spatial analysis function in ArcGIS with a clustering model to select areas on highways that are prone to fogging, thus providing guidance for highway safety strategies and active traffic management.

In respect of microlevel mode, the studies mainly focused on the vehicle itself to provide anticollision function. For example, a networked vehicle collision warning system (CWS) was designed on the basis of connected vehicles. This system used real-time data to predict the collision risk of vehicles and promptly alert drivers to improve the rationality and safety of driver's driving operations [17]. Li [18] developed a control strategy with a variable speed limit (VSL) to reduce the risk of secondary collision during adverse weather. In addition, self-driving vehicles were tested on-site in areas with poor visibility. It was expected that self-driving cars that adapt to various scenarios in the real world would be developed soon [16]. To the best of our knowledge, the current research is aimed at independent human-driven vehicles (HDVs) accident-related behavior analysis or connected automatic vehicles (CAVs) control strategy in dense fog weather conditions, respectively.

Although interest in CAVs has been growing exponentially in recent years, with increasing levels of automation being introduced to newer vehicles, many new technologies are being developed to intelligent infrastructure-based equipment on the smart highway construction [19]. Due to the wide range of potential applications, the objectives, and framework of control, CAVs will significantly enhance the safety, mobility, and efficiency of highway networks, especially in adverse weather conditions. However, the transition to CAVs is going to be a gradual process. It is expected to see a mixed flow of HDVs and CAVs for the next 50 years [20, 21].

A mixed flow of HDVs and CAVs in the traffic flow will lead to a highly heterogeneous traffic management and control environment. The dynamics, safety, and mobility of traffic flow will change due to the mutual interference caused by the performance differences of HDVs and CAVs, especially in adverse weather conditions. Therefore, how to manage and control the mixed traffic flow to improve the safety, mobility, and efficiency will be a consistent issue before the CAVs society fully realize. As the CAVs will be first practically applied in the highway environment, based on the research and development programs of governments and enterprises [22], this paper attempts to propose a fleet control model to manage the mixed flow of CAVs and HDVs passing through the dense fog environment safely on the highway. The main work of this paper is as follows:

(1) A cellular automatic- (CA-) based HDV following model is proposed to analyze the motion characteristics of HDVs in the mixed flow of HDVs and CAVs, along with considering the following behavior of drivers in dense fog weather conditions.

(2) A fleet control model based on the distributed model predictive control (DMPC) algorithm is proposed by using a mathematical modeling method to manage the HDVs and CAVs within the fleet. It attempts to provide a feasible solution for controlling the fleet to improve the mobility and efficiency of highway network in adverse weather conditions, especially in dense fog environment.

In the aspect of dense fog in the highway, the previous researches mostly focused on the association between the driver behavior and traffic accidents by considering the driver's physiology and psychology and environmental factors [12, 23, 24]. This paper focuses on modeling the driver behavior in the fleet mixed with HDVs and CAVs based on the Nagel–Schreckenberg (NaScH) cellular automatic (CA) model, which has advantages in describing the complex behavior and simulating the characteristics of traffic flow under various scenarios and traffic conditions [25–28].

In the aspect of traffic flow control in dense fog environment, the researches were aimed at independent HDVs or CAVs, respectively. This paper aims to manage the fleet mixed with HDVs and CAVs based on DMPC, which is widely used in control engineering and has advantages in dealing with the uncertainty during dynamical optimization and controlling operation, particularly in the area of vehicle dynamics and motion control [29–31].

The rest of the paper is organized as follows. Section 2 presents the assumptions and scenarios of the proposed model and formulates the fleet control model for HDVs and CAVs in dense fog weather conditions. Section 3 analyzes the feasibility and stability of the fleet control model in dense fog environment. The numerical experiments and discussions are presented in Section 4. Section 5 concludes this article with a summary of the contributions and the limitations of the proposed model, as well as the perspectives on future work.

2. Problem Description and Model Formulation

2.1. Problem Description. Given weather and traffic sensors installed along the side of the highway networks, the stability and time delay of communication among vehicle-to-vehicle (V2V) or vehicle-to-infrastructure (V2I) are important factors that influence the safety and robustness in fleet management and control. The highway road alignment, gradient, and surface conditions also influence the mobility and acceleration performance of vehicles in adverse weather conditions. The driver's ability and intention play an important in car-following modeling and characteristics analysis in mixed traffic flow. This paper mainly focuses on the fleet management and control for HDVs and CAVs in dense fog weather conditions. As to restrict influence factors, we assume the following:

(1) The information interaction time delay between V2V or V2I is less than 20 ms. The time delay can be ignored in the CAVs control. The communication is uninterrupted and functional in dense fog weather conditions.

(2) All the drivers in HDVs have the same motivation that pass through dense fog environment safely. The drivers have no significant difference in driving ability. Nobody breaks out of the fleet during passing through the dense fog environment.

(3) The road alignment, gradient, and surface condition of highway in dense fog environment are consistent. The road gradient and surface condition do not affect the mobility and acceleration performance of vehicles during passing through the dense fog environment.

As to improve the traffic flow throughput and driving safety in dense fog weather condition on the highway, the fleet is composed of HDVs and CAVs. In the fleet, HDVs are driven by human completely and have not the capacity of V2I or V2V communication. CAVs are automatically driving and connect with each other. The HDVs are separated by CAVs in the mixed fleet as to reduce the collision risk caused by limited visibility in dense fog environment. The CAVs serve as an automated guided vehicle (AGV) to percept traffic conditions in dense fog environment. The fleet mixed with HDVs and CAVs is shown as Figure 1.

In Figure 1, the sequence numbers of CAVs and HDVs are labeled as the indices i and j, respectively. The number sequence is from the head to tail of the fleet. $i = \{1, 2, 3, \ldots, n\}$. $j = \{1, 2, 3, \ldots, n\}$. n is a natural number. The ith CAV and jth HDV in the fleet are defined as CAV(i) and HDV(j), respectively. If $j = i$, it means that the HDV(j) is following the CAV(i).

2.2. Model Formulation

2.2.1. The State Space Model of CAVs. In the fleet, the speed of CAV(i) and HDV(j) at time t are defined as $v_i(t)$ and $v_j(t)$, respectively. The locations of CAV(i) and HDV(j) at time t are defined as $d_i(t)$ and $d_j(t)$, respectively. The values of $v_j(t)$ and $d_j(t)$ can be detected and transferred by the following CAV. The minimum safety distance (MSD) between CAV(i) and HDV$(j-1)(i=j)$ and between CAV(i) and HDV$(j)(i=j)$ are defined as [32]

$$d_i^*(t) = -\frac{v_i^2(t)}{2 \times a_i(t)} + l_f, \tag{1}$$

$$d_f^*(t) = v_j(t).\gamma - \frac{v_j^2(t)}{2 \times a_j(t)} + l_f, \tag{2}$$

where $a_i(t)$ and $a_j(t)$ are minimum deceleration of the CAV(i) and HDV(j) at time t, respectively; l_f is the critical headway; and γ is the reaction time of drivers.

$s_i^*(t)$ is defined as the equilibrium spacing (ES) between CAV(i) and HDV$(j-1)(i=j)$ at time t, and $s_i^*(t) > d_i^*(t)$ for CAV(i) in the fleet. The ES of the CAVs in the fleet has the same value; that is, $s_i^*(t) = s^*(t)$, $\forall i = \{1, 2, \ldots .n\}$.

Within the fleet, we pursue the CAV following the HDV with the same velocity of HDV and keeping a safety distance in ES. Therefore, the state of CAV(i) within the fleet is defined as

$$X_i := \left[\Delta d_i(\mathrm{t}), \Delta \mathrm{v}_i(t)\right]^T, \tag{3}$$

where $\Delta d_i(t)$ is the distance difference to ES at time t; $\Delta \mathrm{v}_i(t)$ is the speed difference to HDV$(j-1)$ at time t.

$$\Delta d_i(\mathrm{t}) = d_{j-1}(\mathrm{t}) - d_i(\mathrm{t}) - s^*(\mathrm{t}). \tag{4}$$

$$\Delta v_i(t) = v_{j-1}(t) - v_i(t). \tag{5}$$

Putting formulas (4) and (5) into formula (3), the state space model of CAVs within the fleet can be written as

$$X_i'(t) = AX_i(t) + Bu_i(t) + Da_{j-1}(t), \tag{6}$$

where $X_i'(t) = \begin{bmatrix} \Delta d_i'(t) \\ \Delta V_i'(t) \end{bmatrix}$, $\mathrm{A} = \begin{bmatrix} 0 & 1 \\ 0 & 0 \end{bmatrix}$, $B = \begin{bmatrix} 0 \\ -1 \end{bmatrix}$, $D = \begin{bmatrix} 0 \\ 1 \end{bmatrix}$; $\Delta d_i'(t)$ is the first derivative of $\Delta d_i(t)$, $\Delta v_l'(t)$ is

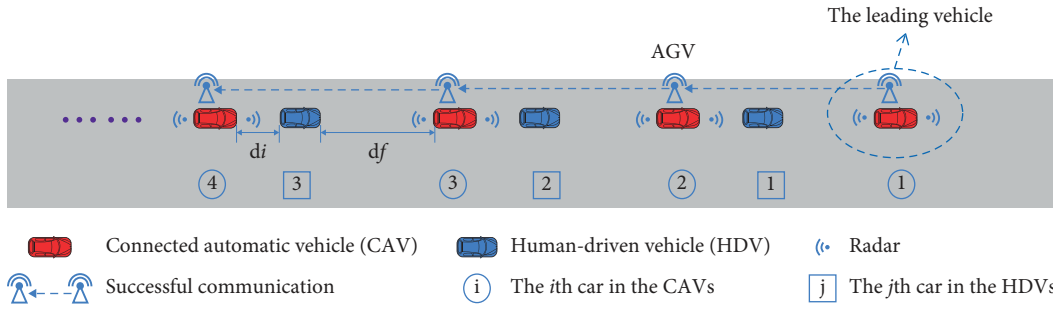

Figure 1: The layout of fleet in dense fog environment.

the first derivative of $\Delta v_i(t)$, $u_i(t)$ is the acceleration of CAV(i) at time t; $a_{j-1}(t)$ is the acceleration of HDV$(j-1)$ at time t; and $j = i$ and $i = \{1, 2, 3, \ldots, n\}$.

As to describe the dynamic state space of CAVs in the fleet control, Δt_s is defined as the discrete sampling time interval, and $\Delta t_s > 0$. K is the discrete sampling time, and $K\Delta t_s \le t \le (K+1)\Delta t_s$. If Δt_s is small enough, the discretization equation can represent the dynamic moving process of CAVs [33, 34]. Therefore, the c2d function in MATLAB is used to disperse the state space of CAVs. The discretization equation is written as

$$X_i(K+1) = A' X_i(K) + B' u_i(K) + D' a_{j-1}(K), \tag{7}$$

where $X_i(K+1) = \begin{bmatrix} \Delta d_i(K+1) \\ \Delta V_i(K+1) \end{bmatrix}$; $X_i(K) = \begin{bmatrix} \Delta d_i(K) \\ \Delta v_i(K) \end{bmatrix}$; $A' = \begin{bmatrix} 2 & \Delta t_s \\ 0 & 1 \end{bmatrix}$; $B' = \begin{bmatrix} -(\Delta^2 t_s/2) \\ -\Delta t_s \end{bmatrix}$; $D' = \begin{bmatrix} \Delta^2 t_s/2 \\ \Delta t_s \end{bmatrix}$; $u_i(K)$ is the acceleration of CAV(i) at time K; $a_{j-1}(K)$ is the acceleration of HDV$(j-1)$ at time K; $j = i$ and $i = \{1, 2, 3, \ldots, n\}$; $K = \{1, 2, 3, \ldots, m\}$; and m is a natural number, $m > 1$.

2.2.2. The Car Following Model of HDVs in Dense Fog Environment on Highway. Rosey [35] found that when the front vehicle is driving at a suitable speed in the dense fog environment, most of the following vehicles will drive and follow within the visibility range. Therefore, in the fleet management, it is important to guide the HDVs to keep safety driving in low-visibility environment by dynamically imposing restrictions on the velocity of AGV in the fleet, as to ensure the AGV always in the vision scope of HDVs and release the nervousness of driver in HDVs. In this situation, modeling the driver behavior of HDVs and the accuracy of car-following model of HDVs in dense fog environment will directly affect the performance of the fleet management, such as feasibility, reliability, stability, and robustness. The cellular automata (CA) model is widely used in traffic flow analysis and has advantages in describing the complex behavior and simulating the characteristics of traffic flow under various scenarios and traffic conditions [25–28]. However, as the CA models in the previous researches mainly focused on interactive between homogeneous vehicles, the current car-following model based on CA cannot be used directly between heterogeneous vehicles environment. Therefore, this paper attempts to model the car-following behavior with a Nagel–Schreckenberg (NaScH) cellular automatic (CA) model to describe the driver behavior in dense fog environment within the fleet mixed with HDVs and CAVs. The model is modeled as follows:

(1) If $d_i(K) - d_j(K) \ge L$ and $i = j$, then HDV driver will accelerate. It means that if the AGV is not in the scope of visibility, the driver of HDV will accelerate carefully to find the AGV [36]. The acceleration action is described as

$$u_j(K) = b \quad (b > 0), \tag{8}$$

where $d_i(K)$, $d_j(K)$ are the location of CAV(i) and HDV(j) at the time K, respectively. L is the distance of visibility in dense fog environment on the highway; b is the random value within a reasonable range of acceleration. The uncertainty of b reflects the randomness of the drivers under the interference of the actual situation.

(2) If $d_i(K) - d_j(K) < L$ and $i = j$, then the HDV driver will make an appropriate adjustment based on the speed and acceleration of HDV and the distance to AGV.

(i) If $d_i(K) - d_j(K) \ge d_f(K)$, then the HDV driver will try to keep pace with the velocity of AGV. That is, if $v_i(t) > v_j(t)$ and $i = j$, the HDV driver will accelerate to keep pace with the AGV; and if $v_i(t) < v_j(t)$ and $i = j$, the HDV driver will decelerate to keep pace with the AGV. The action is described as

$$u_j(K) = u_i(K) + c, \tag{9}$$

where $d_f(K)$ is the MSD between CAV(i) and HDV(j) $(i = j)$ at the time K. c is the random value within a reasonable range of acceleration or deceleration.

(ii) If $d_i(K) - d_j(K) < d_f(K)$, then the HDV driver will decelerate. The deceleration action is described as

$$u_j(K) = f \quad (f < 0), \tag{10}$$

where f is the random value within a reasonable range of deceleration.

Based on the driver behavior described above, the dynamic state of HDVs in the fleet in dense fog environment on the highway can be described as

$$\begin{aligned} v_j(\mathrm{K}+1) &= v_j(\mathrm{K}) + u_j(\mathrm{K}). \\ d_j(\mathrm{K}+1) &= d_j(\mathrm{K}) + v_j(\mathrm{K})\Delta t_s. \end{aligned} \tag{11}$$

We verified the effectiveness of the improved CA model in Section 4.1 and used it as the car-following model of HDVs in the fleet to further verify the fleet control model.

2.2.3. Distributed Model Predictive Control (DMPC). Model Predictive Control (MPC) can deal with the disturbance and uncertainty, and it is widely used in the dynamic vehicle control analysis and simulation [37]. The key difference between MPC and other control methods lies in the use of rolling optimization and rolling implementation of the control function, which makes the MPC more suitable for the complex traffic environments with low visibility. Therefore, CAVs using MPC can respond to the latest status of HDVs at every control moment. On the other hand, in the fleet which is mixed with HDVs and CAVs, it demands for the real-time and dynamical interactive among the CAVs to pass through the dense fog environment safely. As the central communication and control will increase time delay, computation complexity and reduce stability in the fleet control [38], the distributed control mode can take the advantage of CAVs computation, communication ability and reduce the time delay of communication and improve the stability of the system [39]. In addition, according to the layout of the fleet as shown in Figure 1, each CAV has the ability to perform the optimal control by itself. Therefore, this paper attempts to use the distributed model predictive control (DMPC) model to control the fleet in dense fog environment.

The interaction of CAVs within the fleet is described as in Figure 2. In the dense fog environment, the CAVs need to adjust their state according the state of the following HDVs in the fleet. As to adjust the state accurately, CAV (i) needs to obtain the driving state of HDV ($j-1$) from CAV ($i-1$) which can perceive the speed, acceleration, and location of HDV ($j-1$). At time K, CAV ($i-1$) processes the detected historical information, such as locations, speeds of CAV ($i-1$) and HDV ($j-1$). Then, CAV ($i-1$) will calculate the length p and the acceleration of HDV ($j-1$) in the prediction horizon. Furthermore, CAV ($i-1$) will pass the information, such as $d_{j-1}(\mathrm{K})$, $v_{j-1}(\mathrm{K})$, $a_{j-1}(\mathrm{K})$, $a_{j-1}(\mathrm{K}+1)$, ..., $a_{j-1}(\mathrm{K}+\mathrm{p})$ to CAV (i). In synchronization, CAV ($i-1$) completes the optimization control according to the information transmitted by CAV ($i-2$). The optimization control process can be divided into two parts: (1) the fleet state prediction and (2) the fleet control based on DMPC.

(1) The Fleet State Prediction. In the processes of the fleet passing through the dense fog environment, CAV ($i-1$) perceives the speeds and locations of HDV ($j-1$) then evaluates the accelerations of HDV ($j-1$) at the time K. Then, the CAV ($i-1$) transfers these information of HDV ($j-1$) to CAV (i). In addition, CAV ($i-1$) processes the speeds and locations of HDV ($j-1$) before information interaction between CAVs ($j=i$ and $i=\{2, 3, \ldots, n\}$). The CA-based HDVs following model makes the trajectory of HDV ($j-1$) consistent with CAV ($j-1$) in a spatial-temporal delay $\tau_{j-1}(\mathrm{K})$ at time K, as shown in Figure 2. Thus, the locations $d_{j-1}(\mathrm{K}+\rho)$ and speeds $v_{j-1}(\mathrm{K}+\rho)$ of HDV ($j-1$) in prediction horizon can be obtained by dynamical equation. With the spatial-temporal delay $\tau_{j-1}(\mathrm{K})$, the accelerations or decelerations $a_{j-1}(\mathrm{K}+\rho)\,\rho = (0, 1 \ldots . p-1)$ of HDV ($j-1$) in the prediction horizon can be predicted by CAV ($i-1$) based on kinematic equation as

$$\begin{aligned} d_{j-1}(\mathrm{K}+\rho+1) = d_{j-1}(\mathrm{K}+\rho) + \mathrm{v}_{j-1}(\mathrm{K}+\rho)\times\Delta t_s \\ + 0.5\times a_{j-1}(\mathrm{K}+\rho)\times\Delta t_s^2. \end{aligned} \tag{12}$$

The spatial-temporal delay $\tau_{j-1}(\mathrm{K})$ can be obtained by curve matching based on Gong and Du's research [29]. The spatial-temporal delay matching curve is shown in Figure 3.

In Figure 3, it can be seen that there is a critical parameter T_e (time range) in curve matching. And the simulation results showed that if the time range T_e is longer, the more effective information and accurate can be obtained in the prediction. However, the longer time range T_e, the more computation resources are needed in CAVs. As to balance the calculation load and the accuracy of prediction, this paper sets the time range as $T_e = 100$s based on Chen's research [40].

$\{\mathrm{H}_{j,\mathrm{q1}} = (\mathrm{d}_{j,q_\mathrm{h}}, \mathrm{t}_{j,q_\mathrm{h}}), q_\mathrm{h} = 1, 2, 3, \ldots, |\mathrm{H}_j|\}$ and $\{\mathrm{C}_{i,q_\mathrm{c}} = (\mathrm{d}_{i,q_\mathrm{c}}, \mathrm{t}_{i,q_\mathrm{c}}), q_\mathrm{c} = 1, 2, 3, \ldots, |\mathrm{C}_i|\}$ $(i=j)$ are the historical trajectory and current trajectory of HDV (j) and CAV (i), respectively, in Figure 3. $\mathrm{d}_{j,q_\mathrm{h}}$, $\mathrm{t}_{j,q_\mathrm{h}}$ are the location and time of the q_h point in the historical trajectory of HDV (j), respectively. $\mathrm{d}_{i,q_\mathrm{c}}$, $\mathrm{t}_{i,q_\mathrm{c}}$ are the location and time of the q_c point in the current trajectory of CAV (i), respectively. The procedure of spatial-temporal delay matching is described as follows:

Step 1. Find the smallest distance point from C_i to c based on the least square method as

$$\mathrm{D}\left(\mathrm{H}_j, \mathrm{C}_{i,q_\mathrm{c}}\right) = \min\left\|\mathrm{H}_j - \mathrm{C}^2_{i,q_\mathrm{c}}\right\|^2, \tag{13}$$

where $\mathrm{D}(\mathrm{H}_j, \mathrm{C}_{i,q_\mathrm{c}})$ is the minimum distance from the q_c point on C_i to H_j.

Step 2. Calculate the minimum offset of spatial-temporal delay after finding the matching points pair of q_h and q_c in historical trajectory and current trajectory, respectively.

$$\mathrm{MinFt}_\mathrm{I} = \frac{1}{\mathrm{K}_\mathrm{I}}\sum_{\mathrm{K}=1}^{\mathrm{K}_\mathrm{I}}\left\|\mathrm{H}^\mathrm{I}_{j,\mathrm{K}} + \mathbf{t_I} - \mathrm{C}^\mathrm{I}_{i,\mathrm{K}}\right\|^2, \tag{14}$$

where Ft_I is the minimum offset of spatial-temporal delay between C_i and H_j; $(\mathrm{H}^\mathrm{I}_{j,\mathrm{K}}, \mathrm{C}^\mathrm{I}_{i,\mathrm{K}})$ is the K^{th} pairing point in the I^{th} iteration; K_I is the number of matching points in the I^{th} iteration; and $\mathbf{t_I}$ is the delay vector.

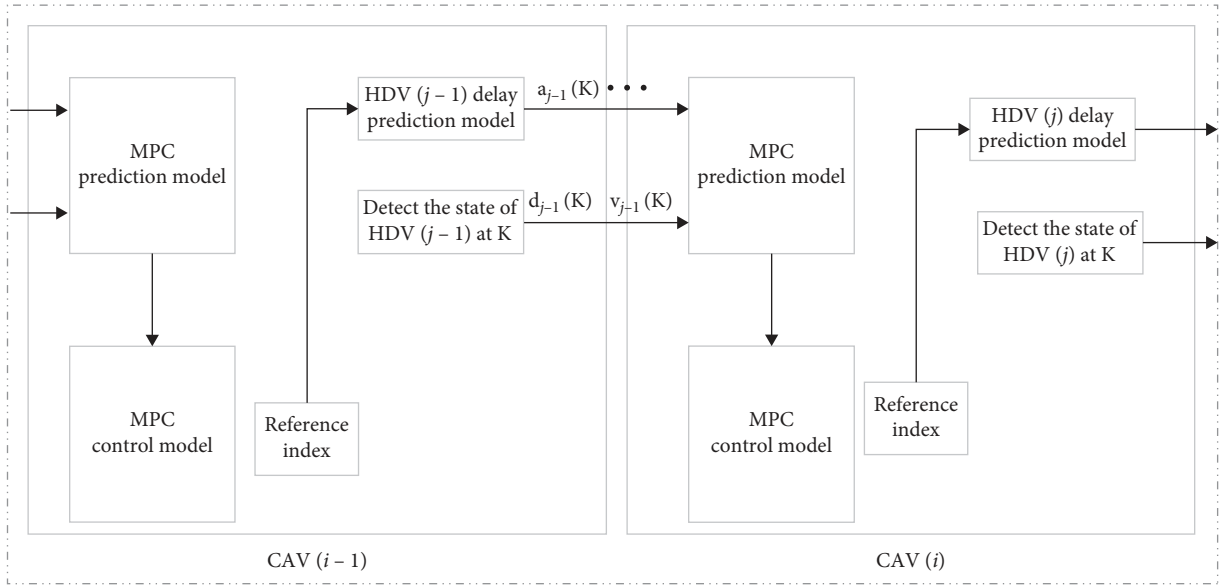

Figure 2: CAVs information interaction and DMPC control in the fleet.

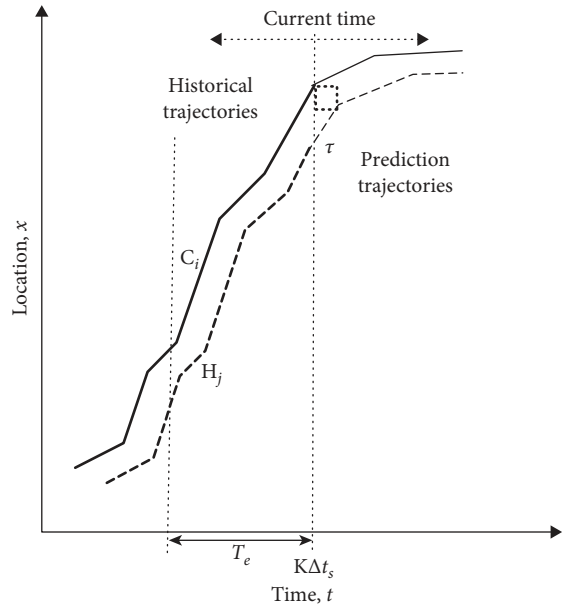

Figure 3: Spatial-temporal delay matching curve for HDV in prediction.

$$\mathbf{t}_{\mathbf{I}}^{*} = -\frac{\sum_{k=1}^{K_I}\left(H_{j,K}^{I} - C_{i,K}^{I}\right)}{K_I}, \tag{15}$$

where t_I^* is the best solution of t_I.

Step 3. Repeat Step 1 and Step 2 until t_I^* is small enough. Then, the HDV (j) trajectory can be predicted by the sum of t_I^* as

$$\left(-\tau_j(K), ds_j(K)\right)^T = \sum t_I^*, \tag{16}$$

where $ds_j(K)$ is the spatial delay of HDV (j) at the time K; $-\tau_j(K)$ is the temporal offset of HDV (j) at the time K.

Then, the length of prediction horizon p of the system at the time K can be calculated as

$$p = \left[\frac{\tau_{j-1}(K)}{\Delta t_s}\right] + 1. \tag{17}$$

(2) The Fleet Control Based on DMPC. In the fleet. CAV (i)*can obtain the following information by information interaction and prediction.*

(1) The location and speed of HDV $(j-1)$ at time K

(2) The accelerations or decelerations of HDV $(j-1)$ in prediction horizon and the length of prediction horizon

CAV (i) obtains these pieces of information to update the state space of the system in horizon prediction and fleet control. In addition, the aim of the fleet control in dense fog environment is passing through the dense fog environment safely and steadily, keeping the vehicles in safety distance and within the scope of visibility. Thus, the object function of the fleet control in dense fog environment can be described as

$$\min J_i(\mathrm{K}) = \sum_{s=1}^{p} \left\{ \left(X_{i,\mathrm{K}+s}^{\mathrm{K}}\right)^T Q_i \left(X_{i,\mathrm{K}+s}^{\mathrm{K}}\right) + R_i \left(u_{i\ \mathrm{K}+s-1}^{\mathrm{K}}\right)^2 \right\} + \left(X_{i,\mathrm{K}+p}^{\mathrm{K}}\right)^T W_i \left(X_{i,\mathrm{K}+p}^{\mathrm{K}}\right), \tag{18}$$

where $X_{i,\mathrm{K}+s}^{\mathrm{K}}$ is the $(\mathrm{K}+\mathrm{s})^{th}$ $(s = (1, 2, \ldots, p))$ state space of the system which is predicted at time K; $u_{i\ \mathrm{K}+s-1}^{\mathrm{K}}$ is the $(\mathrm{K}+\mathrm{s})^{\mathrm{th}}$ control variable which is calculated at time K; $X_{i,\mathrm{K}+p}^{\mathrm{K}}$ is the terminal state space of system which is predicted at time K; and Q_i, R_i are weight matric or weight value, respectively. Q_i is symmetric and positive definite matric, which is usually designed as $\mathrm{Q}_i = \mathrm{diag}(\alpha_{i1}, \alpha_{i2})(\alpha_{i1} > 0, \alpha_{i2} > 0)$; R_i is the coefficient that affects control variable and driver comfort, $\mathrm{R}_i > 0$. Q_i and R_i are the critical coefficient parameters in the fleet control and affect the stability of the fleet.

In formula (18), a comprehensive balanced control method is used to ensure the CAV (i) performing the best operation at time K. It adopts two items to achieve this goal. The first item is $(X_{i,\mathrm{K}+s}^{\mathrm{K}})^T Q_i (X_{i,\mathrm{K}+s}^{\mathrm{K}})$, which attempts to reduce the position and speed errors of CAV (i) and HDV $(j-1)$ during passing through the dense fog environment. And $R_i (u_{i\ \mathrm{K}+s-1}^{\mathrm{K}})^2$ is used to reduce CAV (i)'s energy consumption and improve the comfort. The second item is $(X_{i,\mathrm{K}+m}^{\mathrm{K}})^T W_i (X_{i,\mathrm{K}+m}^{\mathrm{K}})$, which is used to reduce the errors between the state variables and the equilibrium state of the system at the end of the prediction horizon. In this study, W_i is the solution of the discrete algebraic Riccati equation as formula (20), which is used to ensure the local asymptotic stability of the fleet [41].

$$W_i = \mathrm{Q}_i + \mathrm{A}' \left[W_i - W_i B' \left(\mathrm{R}_i + B'^T W_i B' \right)^{-1} B'^T W_i \right] \mathrm{A}'. \tag{19}$$

The constraints of object function in the fleet control are set as follows:

(1) Control constraints:

$$u_{\min} \le u_{i,\mathrm{K}+s}^{\mathrm{K}} \le u_{\max} \quad \forall s \in \{0, 1, 2, \ldots p-1\}. \tag{20}$$

(2) State constraints:

$$v_{\min} \le v_{i,\mathrm{K}+s}^{\mathrm{K}} \le v_{\max} \ \ \forall s \in \{1, 2, 3, \ldots .. p\}, \tag{21}$$

where $v_{\min}$ and $v_{\max}$ are the minimum and maximum speed of the fleet during passing through the dense fog environment on highway, respectively.

$$\Delta d_{i,\mathrm{K}+s}^{\mathrm{K}} + s^*(t) \ge d_i^*(\mathrm{K}+s \mid \mathrm{K}), \tag{22}$$

where $\Delta d_{i,\mathrm{K}+s}^{\mathrm{K}}$ is the $(\mathrm{K}+s)^{\mathrm{th}}$ distance difference of system which is predicted at time K; $d_i^*(\mathrm{K}+s \mid \mathrm{K})$ is the $(\mathrm{K}+s)^{\mathrm{th}}$ MSD of CAV (i) which is predicted at time K.

$$\Delta d_i^- \le \Delta d_{i,\mathrm{K}+s}^{\mathrm{K}} \le \Delta d_i^+ \quad \forall s \in \{1, 2, 3, \ldots p\}, \tag{23}$$

where

$$\begin{aligned} \Delta d_i^- &= -\max\left(\left|\Delta d_{i-1,\sigma}^r\right|\right) \text{for i} > 1 \text{ for} \quad \forall \sigma \in \{1, 2, 3, \ldots, \mathrm{K}\}, \\ \Delta d_i^+ &= \max\left(\left|\Delta d_{i-1,\sigma}^r\right|\right) \text{for i} > 1 \text{ for} \quad \forall \sigma \in \{1, 2, 3, \ldots, \mathrm{K}\}, \end{aligned} \tag{24}$$

where $\Delta d_{i-1,\sigma}^r$ is the actual state of CAV $(i-1)$ at time σ.

The constraint formulas (23) and (24) are used to guarantee the stability of the fleet.

3. Analysis Feasibility and Stability of Fleet Control in Dense Fog Environment

Based on the theory of Lyapunov stability [42, 43], if the fleet is in the status of feasibility, it means that it can find out the optimal control based on the state constraints. Within the feasibility analysis, the stability analysis includes analysis of the asymptotic stability and string stability. The asymptotic stability refers to the ability of the elements in the system to return to the initial stable states in a short period when subjected to slight disturbances. In this paper, it refers to the CAVs in the fleet. And the string stability reflects the ability of the system (the fleet) to resist slight disturbances. Therefore, the feasibility and stability analysis for the fleet is the premise of performing optimal control. Through the analysis, it can tell us whether the optimal control can be found out to keep the fleet stable.

3.1. The Feasibility of Fleet Control. In the fleet control, as to enforce the feasibility of the controller, the controller should have the capability to endure a certain range of disturbances. As to improve the feasibility of the fleet, the constraints of the fleet can be rewritten as

$$\begin{aligned} U = \Big\{ & \mathrm{u}_{i\ \mathrm{K}+s}^{\mathrm{K}} \mid \mathrm{u}_{\min} \le \mathrm{u}_{i\ \mathrm{K}+s}^{\mathrm{K}} \le \mathrm{u}_{\max}, \mathrm{v}_{\min} \le \mathrm{v}_{i\ \mathrm{K}+s}^{\mathrm{K}} \\ & \le \mathrm{v}_{\max}, d_{j-1,\mathrm{K}+s}^{\mathrm{K}} - d_{i,\mathrm{K}+s}^{\mathrm{K}} + \frac{\left(\mathrm{v}_{i,K+s}^{K}\right)^2}{2\mathrm{u}_{\min}} \\ & - l_f \ge 0, \left| d_{j-2,\mathrm{K}+s}^{\mathrm{K}} - d_{i-1,\mathrm{K}+s}^{\mathrm{K}} \right| \ge \left| d_{j-1,\mathrm{K}+s}^{\mathrm{K}} - d_{i,\mathrm{K}+s}^{\mathrm{K}} \right| \Big\}, \end{aligned} \tag{25}$$

where $\mathrm{u}_{i\ \mathrm{K}+s}^{\mathrm{K}}$ is the s^{th} control value of CAV (i) in prediction horizon at time K; $d_{j-1,\mathrm{K}+s}^{\mathrm{K}}$ is the s^{th} location of HDV $(j-1)$ in prediction horizon at time K; $d_{i,\mathrm{K}+s}^{\mathrm{K}}$ is the s^{th} location of CAV (i) in prediction horizon at time K; and $\mathrm{v}_{i,\mathrm{K}+s}^{\mathrm{K}}$ is the s^{th} speed of CAV (i) in prediction horizon at time K, $j = i$ and $i = \{2, 3, \ldots, n\}$ $(n \in R^+)$, $s = (1, 2, \ldots p)$.

Assume that the $(s-1)^{\mathrm{th}}$ optimal control is feasible; then the speed constraint in formula (25) can be obtained as

$$v_{\min} \le v^{\mathrm{K}}_{i,\mathrm{K}+s-1} + \Delta v^{\mathrm{K}}_{i,\mathrm{K}+s-1} \le v_{\max}. \tag{26}$$

Then, the range of $\mathrm{u}_i^{K}{}_{K+s-1}$ can be obtained by writing the formula 26 as

$$\frac{\mathrm{v}_{\min} - \mathrm{v}^{\mathrm{K}}_{i,\mathrm{K}+s-1}}{\Delta t} \le \mathrm{u}_i^{\mathrm{K}}{}_{\mathrm{K}+s-1} \le \frac{\mathrm{v}_{\max} - \mathrm{v}^{\mathrm{K}}_{i,\mathrm{K}+s-1}}{\Delta t}. \tag{27}$$

Define $\mathrm{u}_{v1} = (\mathrm{v}_{\min} - \mathrm{v}^{\mathrm{K}}_{i,\mathrm{K}+s-1}/\Delta \mathrm{t})$ and $\mathrm{u}_{v2} = (\mathrm{v}_{\max} - \mathrm{v}^{\mathrm{K}}_{i,\mathrm{K}+s-1}/\Delta \mathrm{t})$. As the $(s-1)^{\mathrm{th}}$ optimal control is feasible, and $\mathrm{v}_{\min} \le \mathrm{v}^{\mathrm{K}}_{i,\mathrm{K}+s-1} \le \mathrm{v}_{\max}$, it can deduced that $u_{v1} < 0$ and $u_{v2} > 0$. Thus, we can get the control value that satisfies both the acceleration and speed value in the fleet can be restricted to satisfy the constraints and make sure the fleet is feasible.

In addition, as the $(s-1)^{\mathrm{th}}$ optimal control is feasible, the MSD constraint in formula (25) can be obtained as

$$\begin{aligned} & d^{\mathrm{K}}_{j-1,\mathrm{K}+s} - d^{\mathrm{K}}_{i,\mathrm{K}+s} + \frac{\left(\mathrm{v}^{\mathrm{K}}_{i,\mathrm{K}+s}\right)^2}{2\mathrm{u}_{\min}} - l_f = \left(d^{\mathrm{K}}_{j-1,\mathrm{K}+s-1} + \mathrm{v}^{\mathrm{K}}_{j-1,\mathrm{K}+s-1}\Delta \mathrm{t} + \frac{\Delta \mathrm{t}^2}{2} a^{\mathrm{K}}_{j-1,\mathrm{K}+s-1} \right) \\ & - \left(d^{\mathrm{K}}_{i,\mathrm{K}+s-1} + \mathrm{v}^{\mathrm{K}}_{i,\mathrm{K}+s-1}\Delta t + \frac{\Delta t^2}{2} u^{\mathrm{K}}_{i,\mathrm{K}+s-1} \right) + \frac{\left(\mathrm{v}^{K}_{i,K+s-1} + u^{\mathrm{K}}_{i,K+s-1}\right)^2}{2u_{\min}} - l_f = \frac{\Delta t^2}{2u_{\min}} \left(u^{\mathrm{K}}_{i,\mathrm{K}+s-1}\right)^2 \\ & + \left(\frac{\left(v^{\mathrm{K}}_{i,\mathrm{K}+s-1}\Delta t\right)}{u_{\min}} - \frac{\Delta t^2}{2} \right) u^{\mathrm{K}}_{i,\mathrm{K}+s-1} + \left[\left(d^{\mathrm{K}}_{j-1,\mathrm{K}+s-1} - d^{\mathrm{K}}_{i,\mathrm{K}+s-1} \right) \right. \\ & \left. + \Delta \mathrm{t}\left(\mathrm{v}^{\mathrm{K}}_{j-1,\mathrm{K}+s-1} - \mathrm{v}^{\mathrm{K}}_{i,\mathrm{K}+s-1}\right) + \frac{\Delta \mathrm{t}^2}{2} a^{\mathrm{K}}_{j-1,\mathrm{K}+s-1} + \frac{\left(\mathrm{v}^{\mathrm{K}}_{i,\mathrm{K}+s}\right)^2}{2u_{\min}} - l_f \right] = 0, \end{aligned} \tag{28}$$

where $a^{\mathrm{K}}_{j-1,\mathrm{K}+s-1}$ is the $(s-1)^{th}$ control value of HDV $(j-1)$ in prediction horizon at time K; $\mathrm{v}^{K}_{j-1,K+s-1}$ is the $(s-1)^{th}$ speed of HDV $(j-1)$ in prediction horizon at time K.

Given $\mathrm{u}_{\min} < 0$ and $d^{\mathrm{K}}_{j-1,K+s} - d^{\mathrm{K}}_{i,K+s} + ((\mathrm{v}^{K}_{i,K+s})^2/2\mathrm{u}_{\min}) - l_f \ge 0$, then $u^{\mathrm{K}}_{i,K+s-1}$ is between the two roots of formula 30

$$u_{\mathrm{msd1}} = \frac{u_{\min}}{2} + \frac{u_{v1}}{\Delta t} + \frac{u_{\min}}{2\Delta t}\sqrt{C}, \tag{29}$$

$$u_{\mathrm{msd2}} = \frac{u_{\min}}{2} + \frac{u_{v1}}{\Delta t} - \frac{u_{\min}}{2\Delta t}\sqrt{C}, \tag{30}$$

$$C = \frac{\Delta \mathrm{t}^2 u_{\min} + 8\left(l_f - d^{\mathrm{K}}_{j-1,\mathrm{K}+s-1} + d^{\mathrm{K}}_{i,\mathrm{K}+s-1}\right) - 4\Delta \mathrm{t}\left(\mathrm{v}^{\mathrm{K}}_{j-1,\mathrm{K}+s-1} + \mathrm{v}^{\mathrm{K}}_{j-1,\mathrm{K}+s} - \mathrm{v}^{\mathrm{K}}_{i,\mathrm{K}+s-1}\right)}{u_{\min}}. \tag{31}$$

As the $(s-1)^{\mathrm{th}}$ optimal control is feasible, then $l_f - d^{\mathrm{K}}_{j-1,\mathrm{K}+s-1} + d^{\mathrm{K}}_{i,\mathrm{K}+s-1} < 0$. If the control interval $\Delta \mathrm{t}$ is small enough, the vehicles in the fleet will have little difference in speed. Thus, $\mathrm{v}^{\mathrm{K}}_{j-1,\mathrm{K}+s-1} + \mathrm{v}^{\mathrm{K}}_{j-1,\mathrm{K}+s} - \mathrm{v}^{\mathrm{K}}_{i,\mathrm{K}+s-1} > 0$, $A > 0$, and $\mathrm{u}_{\mathrm{msd1}} < \mathrm{u}_{\mathrm{msd2}}$.

$$\begin{aligned} \mathrm{u}_1 &= \max\left(\mathrm{u}_{\min,}\, \mathrm{u}_{v1},\, \mathrm{u}_{\mathrm{msd1}}\right), \\ \mathrm{u}_2 &= \min\left(\mathrm{u}_{\max}, \mathrm{u}_{v2},\, \mathrm{u}_{\mathrm{msd2}}\right), \end{aligned} \tag{32}$$

where u_1 is the lower boundary of the constraint; u_2 is the upper bound of the constraint.

Given $u_{v1} < 0 u_{\min} < 0$, and $0 < \Delta t < 1$, the change of u_{v1} can be obtained as

$$u_{\mathrm{msd1}} < \frac{u_{v1}}{\Delta t} < u_{v1}. \tag{33}$$

Then, $u_1 = \max(u_{\min,}\, u_{v1})$ according to formula (33). Based on formulas (1), (22), (27), (30), and (31), the range of u_{msd2} can be obtained as

$$\begin{aligned} u_{\mathrm{msd2}} &\ge \frac{u_{\min}\Delta t + 2u_{v1} + \sqrt{\Delta t^2 u_{\min}^2 + 8u_{v1}^2 + 4\Delta t^2 u_{\min} u_{v1}}}{2\Delta t} \\ &> \frac{u_{\min}\Delta t + 2u_{v1} + \left|u_{\min}\Delta t + 2\sqrt{2}\, u_{v1}\right|}{2\Delta t} > 0. \end{aligned} \tag{34}$$

Thus, $u_{\mathrm{msd2}} > u_{v1}$ and $u_{\mathrm{msd2}} > u_{\min}$. If $u_{v1} < 0$ and $u_{\min} < 0$, then $u_2 > u_1$. It can be concluded that the first three constraints in formula (25) are feasible.

Next, it can be found that the fourth constraint in formula (25) makes the constraint (25) loose. That is due to the fact that $|d^{\mathrm{K}}_{j-2,\mathrm{K}+s} - d^{\mathrm{K}}_{i-1,\mathrm{K}+s}| > (-((v^{\mathrm{K}}_{i-1,\mathrm{K}+s})^2/2u_{\min}) + l_f)$, which $\left\{(-(v^{\mathrm{K}}_{i-1,\mathrm{K}+s})^2/2u_{\min})\right\}$ is approximately equal to $(-(v^{\mathrm{K}}_{i,\mathrm{K}+s})^2/2u_{\min})$ when the fleet is running normally. Thus, the fourth constraint is more relaxed than the third constraint in formula (25). In other words, the controller rolling

optimization at the control time is feasible under a certain range of disturbances.

3.2. The Stability Analysis for Fleet Control. Stability is an important feature for the fleet. In this study, we analyze the asymptotic stability of the single system and the string stability of the formation. According to the theorem developed by Mayne [44], Zhou [30], and the Lyapunov stability principle [42, 43], if the optimal control meets the following five conditions, the asymptotic stability of the system can be guaranteed:

(1) $X_{i,e} \in Z_f$

(2) $\mathrm{K}_f(X^{\mathrm{K}}_{i,\mathrm{K}+s}, a^{\mathrm{K}}_{j-1,\mathrm{K}+s}) \in \mathrm{U} \quad \forall X^{\mathrm{K}}_{i,\mathrm{K}+s} \in Z_f$

(3) $\mathrm{A}' X^{\mathrm{K}}_{i,\mathrm{K}+s} + B'\mathrm{K}_f(X^{\mathrm{K}}_{i,\mathrm{K}+s}, a^{\mathrm{K}}_{j-1,\mathrm{K}+s}) + D' a^{\mathrm{K}}_{j-1,\mathrm{K}+s} \in X_f, \quad \forall X^{\mathrm{K}}_{i,\mathrm{K}+s} \in Z_f$

(4) $\mathrm{F}(\mathrm{A}' X^{\mathrm{K}}_{1,\mathrm{K}+\mathrm{p}} + B'\mathrm{K}_f(X^{\mathrm{K}}_{1,\mathrm{K}+\mathrm{p}})) - \mathrm{F}(X^{\mathrm{K}}_{1,\mathrm{K}+\mathrm{p}}) + \mathrm{L}(\mathrm{A}' X^{\mathrm{K}}_{1,\mathrm{K}+\mathrm{p}} + B'\mathrm{K}_f(X^{\mathrm{K}}_{1,\mathrm{K}+\mathrm{p}})) \le 0 \quad X^{\mathrm{K}}_{1,\mathrm{K}+\mathrm{p}} \in Z_f$ and

(5) $\mathrm{CAV}(i)$ is robust recursive feasibility, $\forall i \in (2, 3, \ldots n)$.

Here, $X_{i,e}$ is the equilibrium state; Z_f is the terminal state domain; K_f is the implicit control law; F, L are the cost functions, respectively. The other symbols have the same meaning as above.

Z_f is set as a subset of the robust invariant set according to Zhou [30] as

$$i, \mathrm{RIS} = \left\{ X^{K}_{i,\mathrm{K}+s} = \left[\Delta \mathrm{d}^{\mathrm{K}}_{i,\mathrm{K}+s}, \Delta \mathrm{v}^{\mathrm{K}}_{i,\mathrm{K}+s}, a^{\mathrm{K}}_{j-1,\mathrm{K}+s}\right] \subseteq i, \mathrm{RIS} \,\middle|\, \mathrm{A}' X^{\mathrm{K}}_{i,\mathrm{K}+s} + B'\mathrm{K}_f\left(X^{\mathrm{K}}_{i,\mathrm{K}+s}, a^{\mathrm{K}}_{j-1,\mathrm{K}+s}\right) + D' a^{\mathrm{K}}_{j-1,\mathrm{K}+s} \in i, \mathrm{RIS}, \mathrm{K}_f\left(X^{\mathrm{K}}_{i,\mathrm{K}+s}, a^{\mathrm{K}}_{j-1,\mathrm{K}+s}\right) \in \mathrm{U} \text{ and } a^{\mathrm{K}}_{j-1,\mathrm{K}+s} \in \mathrm{U} \right\}. \tag{35}$$

Obviously, $X_{i,e} \in i, \mathrm{RIS}$ and let $Z_f \subseteq i, \mathrm{RIS}$; then, conditions (1), (2), and (3) as mentioned above are fulfilled. According to formula (7) and formula (18), condition (4) can be reorganized as

$$\begin{aligned} &\left(\mathrm{A}' X^{\mathrm{K}}_{1,\mathrm{K}+\mathrm{p}} + B'\mathrm{K}_f\left(X^{\mathrm{K}}_{1,\mathrm{K}+\mathrm{p}}\right)\right)^T W_i \left(\mathrm{A}' X^{\mathrm{K}}_{1,\mathrm{K}+\mathrm{p}} + B'\mathrm{K}_f\left(X^{\mathrm{K}}_{1,\mathrm{K}+\mathrm{p}}\right)\right) - \left(X^{\mathrm{K}}_{1,\mathrm{K}+\mathrm{p}}\right)^T W_i \left(X^{\mathrm{K}}_{1,\mathrm{K}+\mathrm{p}}\right) \\ &+ \left(\mathrm{A}' X^{\mathrm{K}}_{1,\mathrm{K}+\mathrm{p}} + B'\mathrm{K}_f\left(X^{\mathrm{K}}_{1,\mathrm{K}+\mathrm{p}}\right)\right)^T Q_i \left(\mathrm{A}' X^{\mathrm{K}}_{1,\mathrm{K}+\mathrm{p}} + B'\mathrm{K}_f\left(X^{\mathrm{K}}_{1,\mathrm{K}+\mathrm{p}}\right)\right) + R_i \left(\mathrm{K}_f\left(X^{\mathrm{K}}_{i,\mathrm{K}+\mathrm{p}}, a^{\mathrm{K}}_{j-1,\mathrm{K}+\mathrm{p}}\right)\right)^2 \le 0. \end{aligned} \tag{36}$$

Assume the implicit control law $\mathrm{K}_f(X^{\mathrm{K}}_{1,\mathrm{K}+s}) = kX^{\mathrm{K}}_{1,\mathrm{K}+s}$ ($s = (1, 2, \ldots, p)$, formula (36) can be rewritten as

$$\begin{aligned} &\left(X^{\mathrm{K}}_{1,\mathrm{K}+\mathrm{p}}\right)^T \left\{ (\mathrm{A}' + B'k)^T W_i (\mathrm{A}' + B'k) - W_i \right. \\ &\left. + (\mathrm{A}' + B'k)^T Q_i (\mathrm{A}' + B'k) + R_i k \right\} \left(X^{K}_{1,\mathrm{K}+\mathrm{p}}\right) \le 0. \end{aligned} \tag{37}$$

Let $\vartheta = (\mathrm{A}' + B'k)^T W_i (\mathrm{A}' + B'k) - W_i + (\mathrm{A}' + B'k)^T Q_i (\mathrm{A}' + B'k) + R_i k$ and $k = 0$; the first three conditions are also satisfied and ϑ will be simplified as

$$\vartheta = (\mathrm{A}')^T W_i (\mathrm{A}') - W_i + (\mathrm{A}')^T Q_i (\mathrm{A}'), \tag{38}$$

where $A' = \begin{bmatrix} 2 & \Delta t_s \\ 0 & 1 \end{bmatrix}$; $Q_i = \mathrm{diag}(\alpha_{i1}, \alpha_{i2})$. Let $W_i = \mathrm{diag}(\beta_{i1}, \beta_{i2})$; then ϑ can be rewritten as

$$\vartheta = \begin{bmatrix} 3\beta_{i1} + 4\alpha_{i1}, & 2\Delta t_s \beta_{i1} + 2\Delta t_s \alpha_{i1}, \\ 2\Delta t_s \beta_{i1} + 2\Delta t_s \alpha_{i1}, & \Delta t_s^2 \beta_{i1} + \Delta t_s^2 \alpha_{i1} + \alpha_{i2}. \end{bmatrix}. \tag{39}$$

If ϑ is a negative semidefinite matrix, ϑ satisfies the conditions as follows:

$$3\beta_{i1} + 4\alpha_{i1} \le 0, \tag{40}$$

$$\begin{aligned} &(3\beta_{i1} + 4\alpha_{i1})\left(\Delta t_s^2 \beta_{i1} + \Delta t_s^2 \alpha_{i1} + \alpha_{i2}\right) \\ &- \left(2\Delta t_s \beta_{i1} + 2\Delta t_s \alpha_{i1}\right)^2 \ge 0. \end{aligned} \tag{41}$$

It can be deduced that formula (36) will be proved under formula (40). Furthermore, as the appropriate weight matrixes Q, w, and R are selected, formula (36) can be guaranteed in different K_f which satisfies conditions (1), (2), and (3) as mentioned above. Thus, the above four conditions have proved to be feasible; it can be concluded that the single system of fleet is asymptotically stable.

As to prove $\mathrm{CAV}(i)$ is robust recursive feasibility, it should be ensured that CAVs can predict HDVs accurately and interact successfully between CAVs. In the stability theory of dynamical systems, the string stability is well known as the higher level of formation control, which requires the control error gradually decreasing during the formation propagation. Based on the constraints of the object function of fleet control in dense fog environment, it can further set the constraint to meet the string stability as

$$\left|\Delta d^{\mathrm{K}}_{i,\mathrm{K}+s}\right| \le \max\left(\left|\Delta d^{r}_{i-1,\sigma}\right|\right), \tag{42}$$

where $\Delta d^{K}_{i,K+s}$ is the control error of state space at the time $K + s$ which is predicted by of CAV (i) at the time K.

In the restriction in execution, DMPC-based fleet executes the first control variable in each time; $\Delta d^{K}_{i,K+s}$ can be defined as

$$\Delta d^{K}_{i,K+1} = \Delta d^{r}_{i,K+1}. \tag{43}$$

Then, formula (29) can be replaced as

$$\Delta d^{r}_{i,K+1} \leq \max\left(\left|\Delta d^{r}_{i-1,\sigma}\right|\right). \tag{44}$$

If the restrictions in formula (44) are adopted in the fleet control, the fleet will be consistent with the performance of CAVs formation. The control error can gradually decrease in the fleet during the formation propagation [11]. However, in the fleet, the uncertainty and randomness are generated by HDVs drivers. The CAVs following the HDVs need a greater control action to compensate the uncertainty and randomness made by the HDVs drivers. The string stability between CAVs can ensure the global asymptotic stability by reducing the control error during the formation propagation. Therefore, the fleet control in this paper can provide a nonstrict string stability during passing through dense fog environment on the highway.

4. Numerical Experiments

As to verify the performance of fleet in dense fog environment on highway, this paper uses numerical experiments to analyze the ability and capability of fleet with the proposed control model. Firstly, we verified the effectiveness of the improved HDV car-following model; that is, the model can reflect the driving characteristics of the driver in a dense fog environment condition. Secondly, we discussed the driving conditions of the fleet under different visibility to verify the feasibility and asymptotic stability of DMPC. Then, we changed the order of HDVs in the fleet and further analyzed the effective ability of the DMPC-based control model. Finally, we studied the relationship between string stability and control requirements for the fleet. The numerical experiments are performed by MATLAB R2018b on Windows 10 with Intel® Core™ i5-6200U CPU @ 2.30 GHz RAM 4.00 GB.

4.1. The CA-Based NaScH Car following Model Verification. Whether the HDV car-following model meets the driving characteristics of drivers in dense fog weather conditions is the first most important factor in managing and controlling the fleet mixed with HDVs and CAVs efficiently and precisely. Siebert and Wallis [45] had studied "how speed and visibility influence preferred headway distances in highly automated driving." Based on the study of Siebert and Wallis on the relationship between visibility and speed, the proposed car-following model is verified in three parameters groups. The parameters setting in the car-following model is shown in Table 1. V_L is the limited speed of fleet in the visibility L. The initial headway between CAVs and HDVs in the fleet is set equal to the visibility L in the simulation. The random value of b, c, and f is generated by the MATLAB random function within a defined range in Table 1.

It can be seen from Figures 4(c), 4(f), and 4(i) there is no significant different in acceleration characteristics in CAVs or HDVs under different visibility conditions. The control behavior of CAVs and HDVs seems to have the same characteristics. It means that the proposed car-following model can describe the characteristics of HDVs drivers trying to keep pace with AGV in the dense fog environment within the fleet. Based on this characteristic, the HDVs trajectories are following the CAVs trajectories in the fleet in different visibility conditions, as shown in Figures 4(a), 4(d), and 4(g). As to follow up the AGV within the scope of visibility, the HDV driver tries to keep pace with the speed of AGV by dynamically accelerate up or decelerate down the HDV, as shown in Figures 4(b), 4(e), and 4(h), corresponding to Figures 4(c), 4(f), and 4(i), respectively. It is worth noting that there is an acceleration behavior at the initial stage of HDV speed diagram in Figures 4(b), 4(e), and 4(h). It is due to the fact that the initial headway in the fleet is set equal to the distance of visibility. AGV is in the edge of visibility. Therefore, the HDV driver accelerates to keep pace with the AGV. The CA-based NaScH car-following model can reflect this phenomenon. As shown in Figure 4, the trajectory, speed, and acceleration of HDVs are keeping pace with the AGV in the dense fog environment within the fleet.

As to further verify the effectiveness of the proposed car-following model in the dense fog environment with the distance of visibility as 70 m, the initial headway is set as 30 m, 50 m, and 70 m in the verification simulation, respectively. In this situation, 30 m is less than the MSD. 50 m is a little more than the MSD. 70 m is equal to the distance of visibility. As shown in Figure 3, if the initial headway is 30 m, HDV will slow down to keep always from the AGV until the distance is in the safety distance. If the initial headway is 70 m, HDV will accelerate to keep pace with AGV and keep the AGV within the scope of visibility. If the initial headway is 50 m, the HDV will maintain the following state to keep the AGV within the scope of visibility and keep a safety distance from the AGV. The proposed car-following model also reflects these characteristics of HDVs drivers in the dense fog environment within the fleet.

From the phenomena shown in Figures 4 and 5, they are consistent with the assumptions of HDV driver characteristics discussed above and falls into the relationship of speed and visibility as studied by Siebert and Wallis [45]. Therefore, the proposed car-following model above can effectively describe the driver behavior within dense fog environment in the fleet control.

4.2. The DMPC-Based Fleet Control Model Verification. In this section, we focus on verifying the feasibility and stability of the mixed flow of HDVs and CAVs within the fleet. In the fleet, three CAVs and three HDVs are used to form the fleet in the numerical experiments. CAV alternates with HDV in the fleet. That is, the first, third, and fifth are CAV vehicles, and the second, fourth, and sixth are HDV vehicles. Three limited visibility ranges in dense fog environment are used as the fleet scenarios on the highway. The

Table 1: The parameters in the car-following model of HDVs.

Parameter	L (m)	V_L (m/s)	b	c	f	d_f (m)	Initial headway (m)
Simulation 1	40	11	(1, 2)	(−0.5, 0.5)	(−1, 0)	21	40
Simulation 2	60	17	(1, 3)	(−0.5, 0.5)	(−1, 0)	37	60
Simulation 3	70	19	(1, 3)	(−0.5, 0.5)	(−1, 0)	44	70

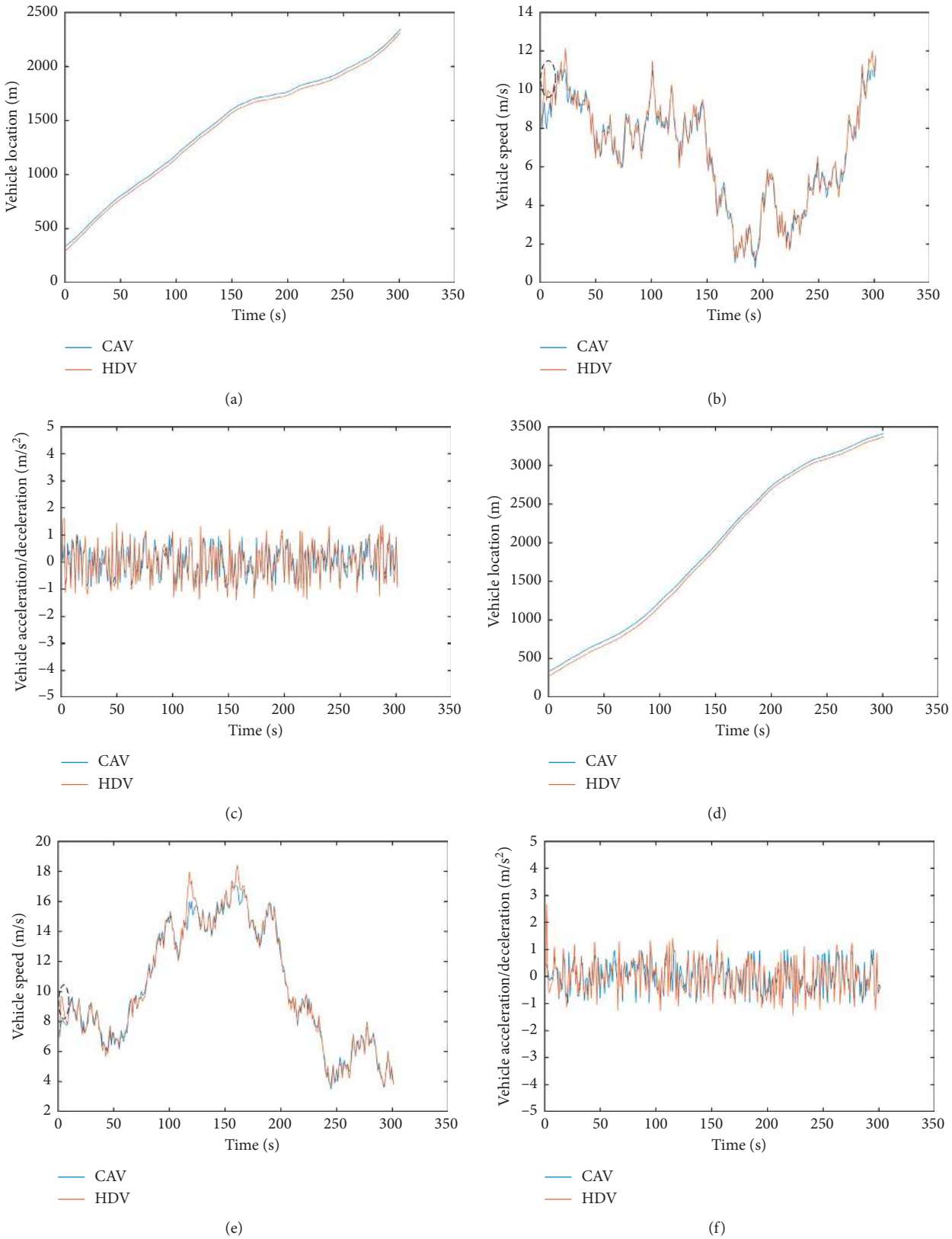

Figure 4: Continued.

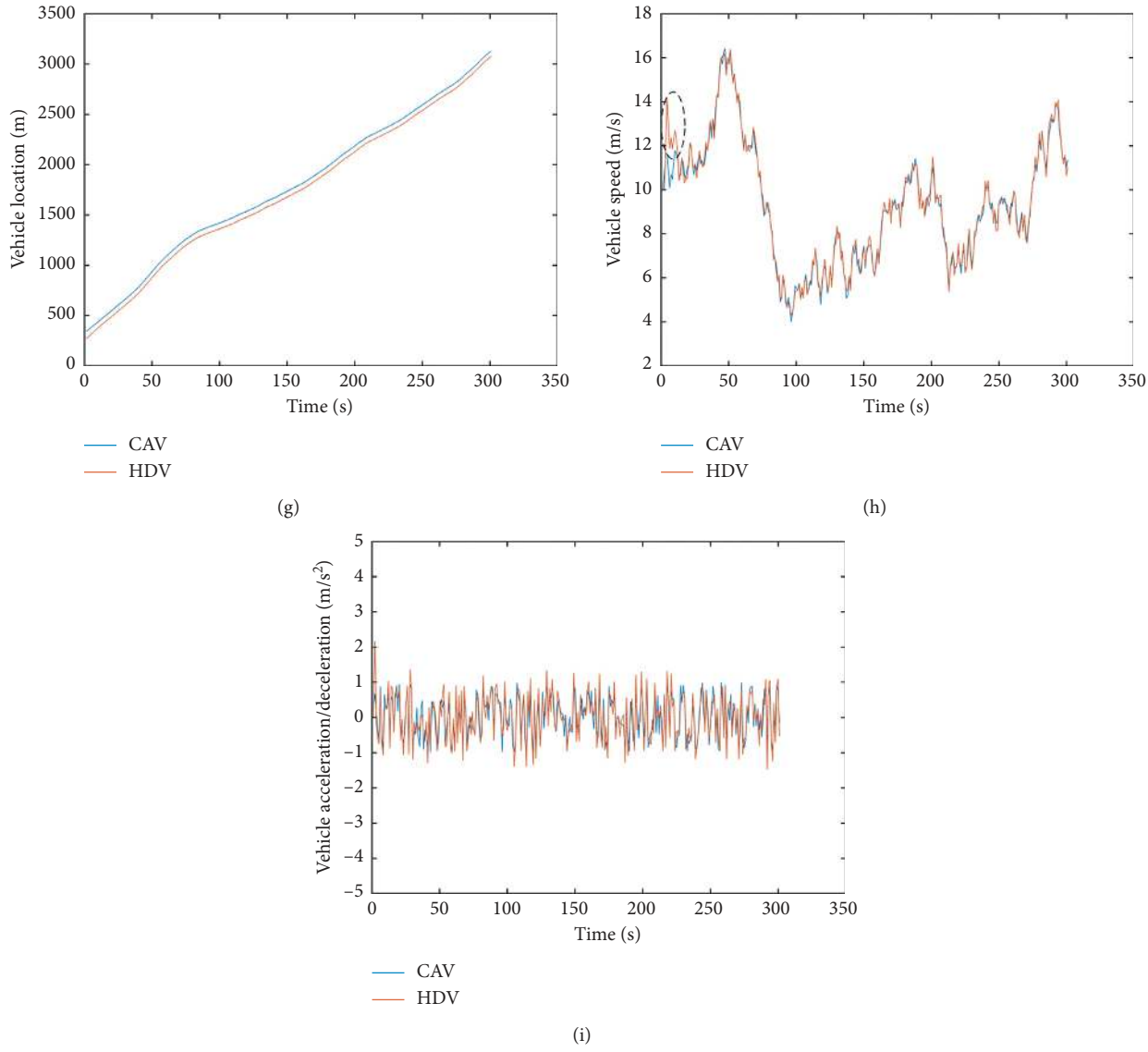

Figure 4: The car-following behavior of HDVs in the fleet within dense fog environment on highway. (a) The vehicle location of CAVs and HDVs ($L = 40$ m). (b) The vehicle speed of CAVs and HDVs ($L = 40$ m). (c) The vehicle acceleration of CAVs and HDVs ($L = 40$ m). (d) The vehicle location of CAVs and HDVs ($L = 60$ m). (e) The vehicle speed of CAVs and HDVs ($L = 60$ m). (f) The vehicle acceleration of CAVs and HDVs ($L = 60$ m). (g) The vehicle location of CAVs and HDVs ($L = 70$ m). (h) The vehicle speed of CAVs and HDVs ($L = 70$ m). (i) The vehicle acceleration of CAVs and HDVs ($L = 70$ m).

parameters setting in the numerical experiments are shown in Table 2.

In the control performance as shown in Figures 6(a), 6(b), 7(a), 7(b), 8(a), and 8(b), CAVs can be basically consistent with the HDVs in trajectory and speed under different driving states, which shows that the controller can guarantee the safe operation of the fleet. Furthermore, as shown in Figures 6(c), 7(c), and 8(c), the spacing in the fleet is controlled within the safety distance under different visibilities. It illustrates that the DMPC prediction model can accurately predict the states of HDVs and passes the information to the rear CAVs. On the other hand, the fleet can maintain the ideal distance between CAVs and HDVs under random disturbance. It shows that the system can ensure asymptotic stability. It should be noted that the continuous fluctuation of the states in the experiments is the result of the joint effect of the experimental inputs and the randomness of HDVs.

4.3. Further Verification by Adjusting the Order of HDVs and CAVs in the Fleet. As to further test the mixed flow of HDVs and CAVs and find out which layouts of the fleet have better performance by the DMPC-based control model, we changed the following number of HDVs between CAVs to two HDVs, three HDVs, and four HDVs in the fleet, respectively. We call these as regular alignment of the fleet, as shown in Figure 9. Then, we changed the queue of the fleet with one HDV between CAVs and three HDVs between

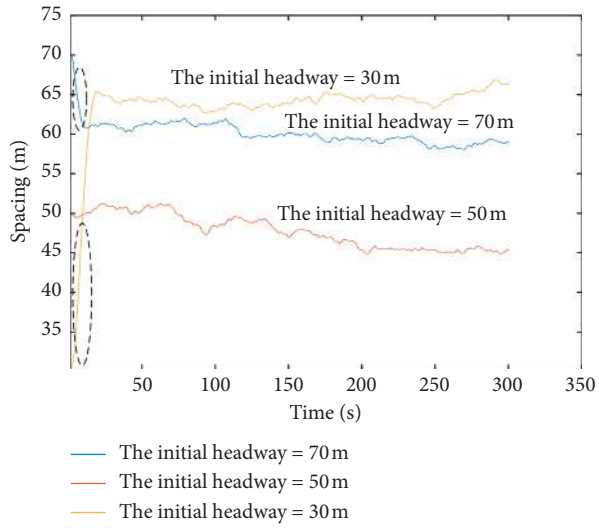

Figure 5: The distance between HDVs and CAVs in different initial headway under the distance of visibility = 70 m in dense fog environment on highway.

Table 2: The parameters in the numerical experiments.

Visibility(m)	V_L(m/s)	b(m)	c(m)	f(m)	d_j^* (m)	d_i^* (m)
50	14	(1,2)	(−0.5,0.5)	(−0.5,0)	28	14
70	19	(1,3)	(−0.5,0.5)	(−1,0)	44	20
90	25	(1,4)	(−0.5,0.5)	(−2,0)	66	41

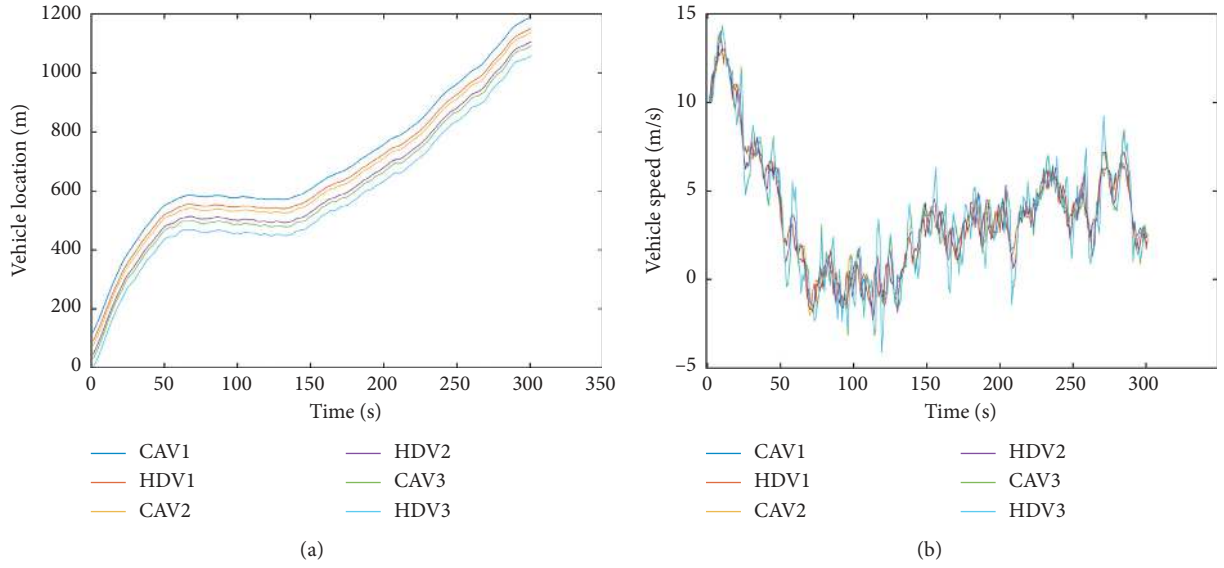

Figure 6: Continued.

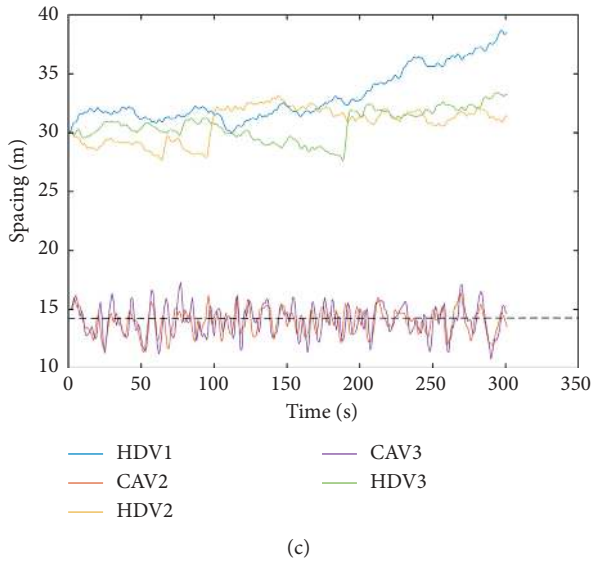

(c)

Figure 6: The fleet in dense fog environment with the visibility being 50 m. (a) The location of formation. (b) The speed of formation. (c) The spacing of formation.

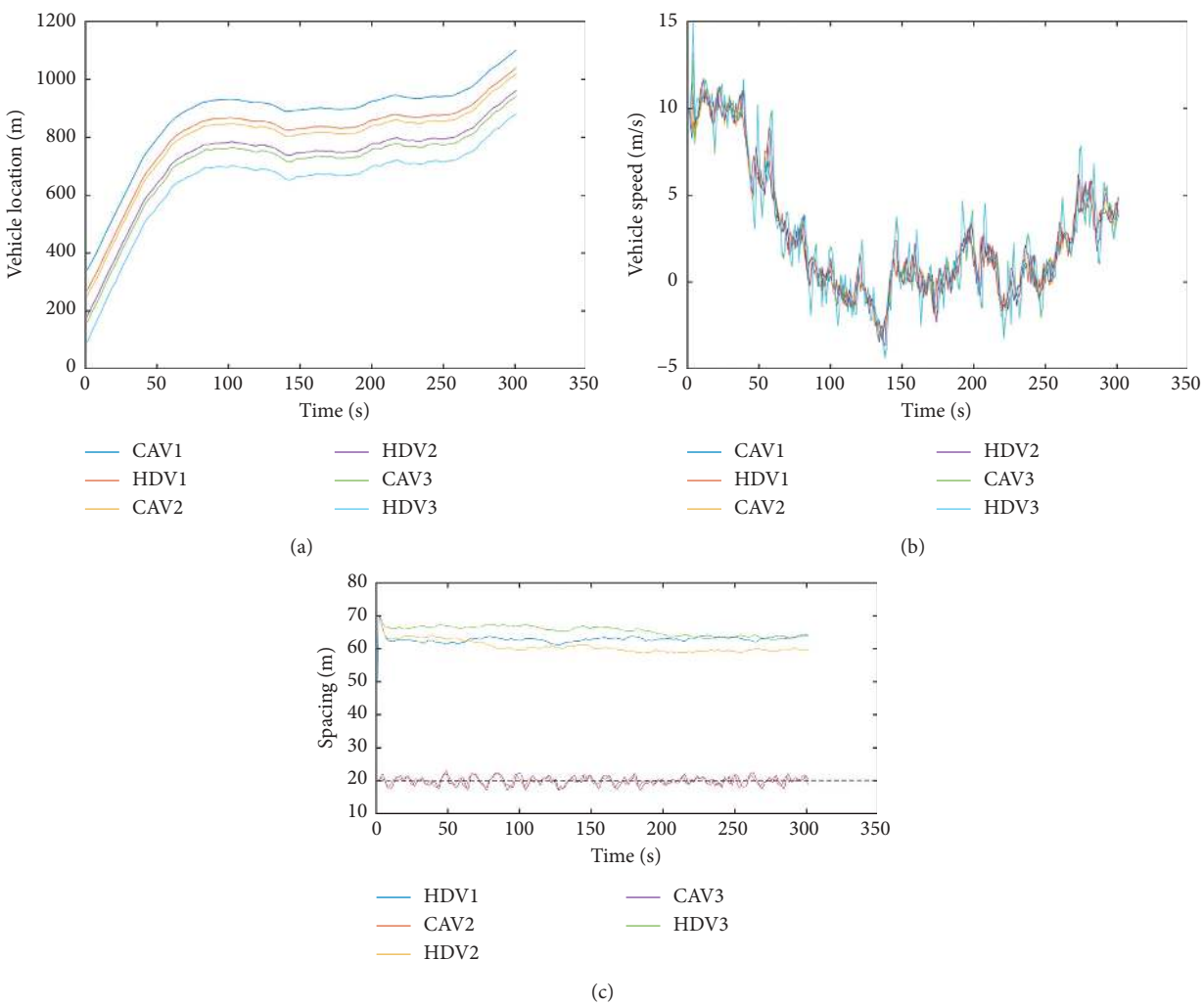

(a)

(b)

(c)

Figure 7: The fleet in dense fog environment with the visibility being 70 m. (a) The location of formation. (b) The speed of formation. (c) The spacing of formation.

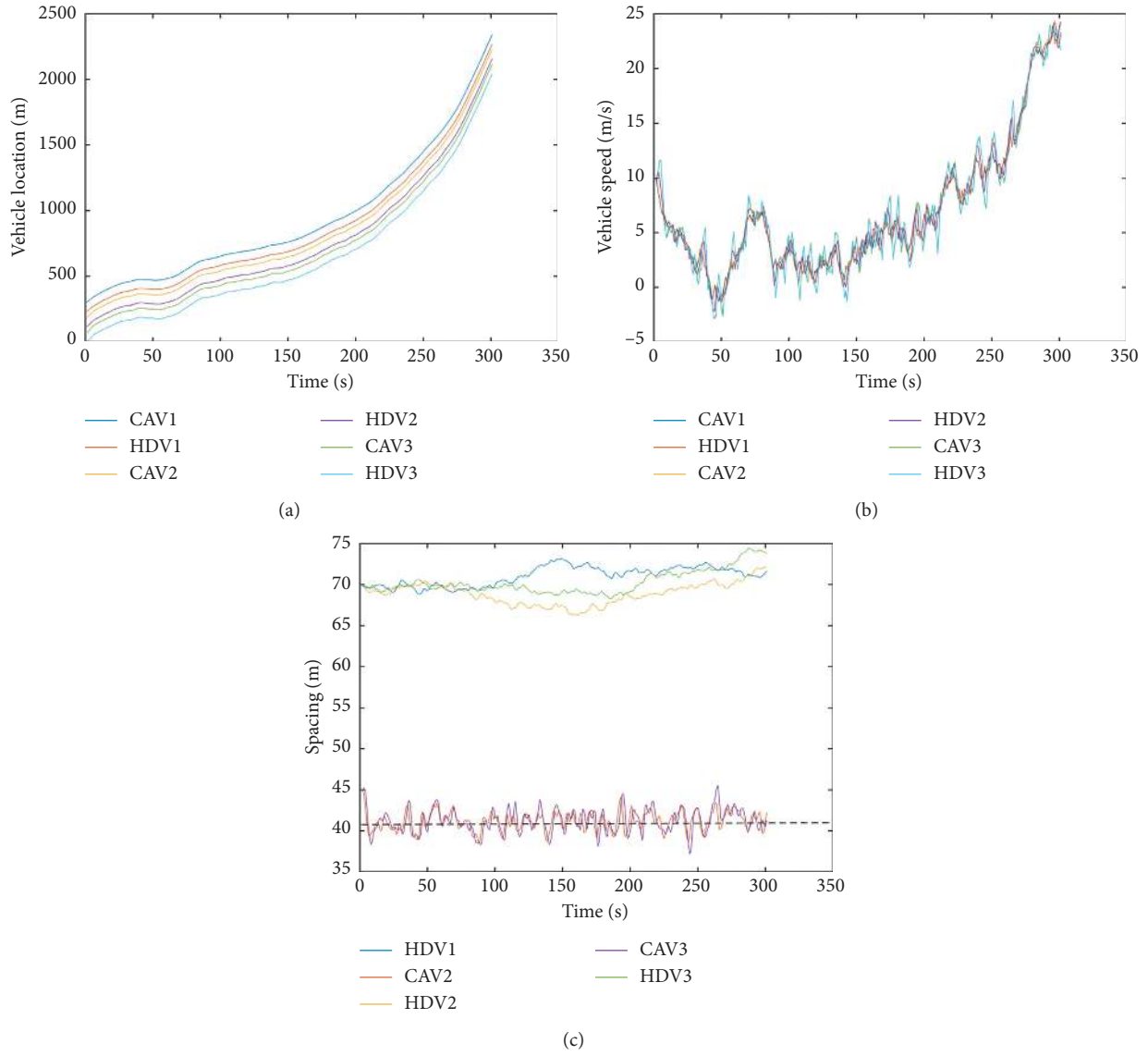

Figure 8: The fleet in dense fog environment with the visibility being 90 m. (a) The location of formation. (b) The speed of formation. (c) The spacing of formation.

CAVs. We call this as irregular alignment of the fleet, as shown in Figure 10. The car-following model between HDVs still used the NaScH CA-based car-following model in the experiments.

Based on the NaScH CA-based car-following model of HDV and the DMPC-based control model, the fleet in the experiments which have different regular alignment or irregular alignment were all can drive normally, as shown in Figures 11(a), 11(b), 11(d), 11(e), 11(g), and 11(h). However, as the number of HDVs between the CAVs within the fleet is increasing, the uncertainty of the fleet is also increasing. For example, by comparing among Figures 11(b), 11(e), and 11(h), it can be seen that as the number of HDVs between the CAVs within the fleet increases to two or three HDVs, the speed volatility of the fleet increases significantly.

In addition, the randomness of HDVs will be transmitted and accumulated between the adjacent HDVs. As shown in Figures 11(c), 11(f), 11(i), and (12), when the preceding vehicles in adjacent HDVs tend to travel at a higher speed and maintain an MSD from the preceding vehicles, the following vehicles in adjacent HDVs also have the same tendency. And the spacing fluctuation of the CAVs after the HDVs is clearly larger than that of the front CAVs. It is worth noting that the NaScH CA-based car-following model does not include aggressive drivers. If there are aggressive drivers in the fleet, it will be difficult to control and optimize the fleet. That is, the higher the penetration rates of CAV in the formation, the more effective the DMPC-based control model.

4.4. The Stability of Fleet Control Verification. Finally, the relationship between string stability and control quality is checked. The relationship checking is carried out under the dense fog environment with the visibility being 70m. The

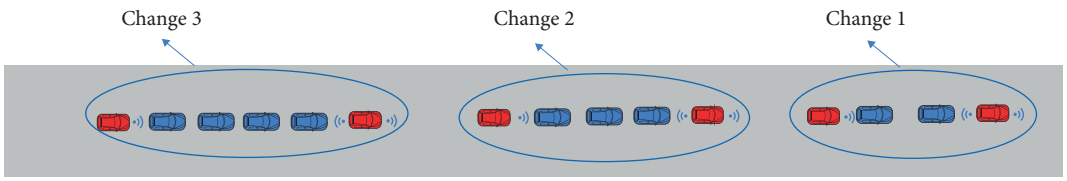

Figure 9: The regular alignment of the fleet.

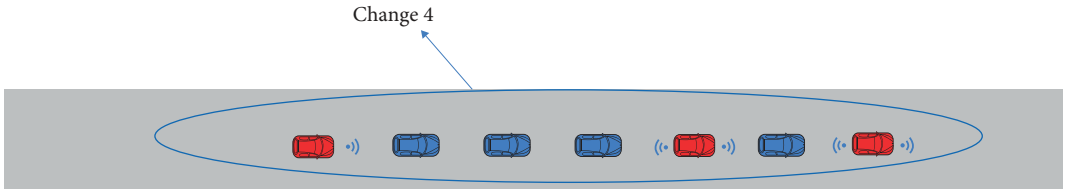

Figure 10: The irregular alignment of the fleet.

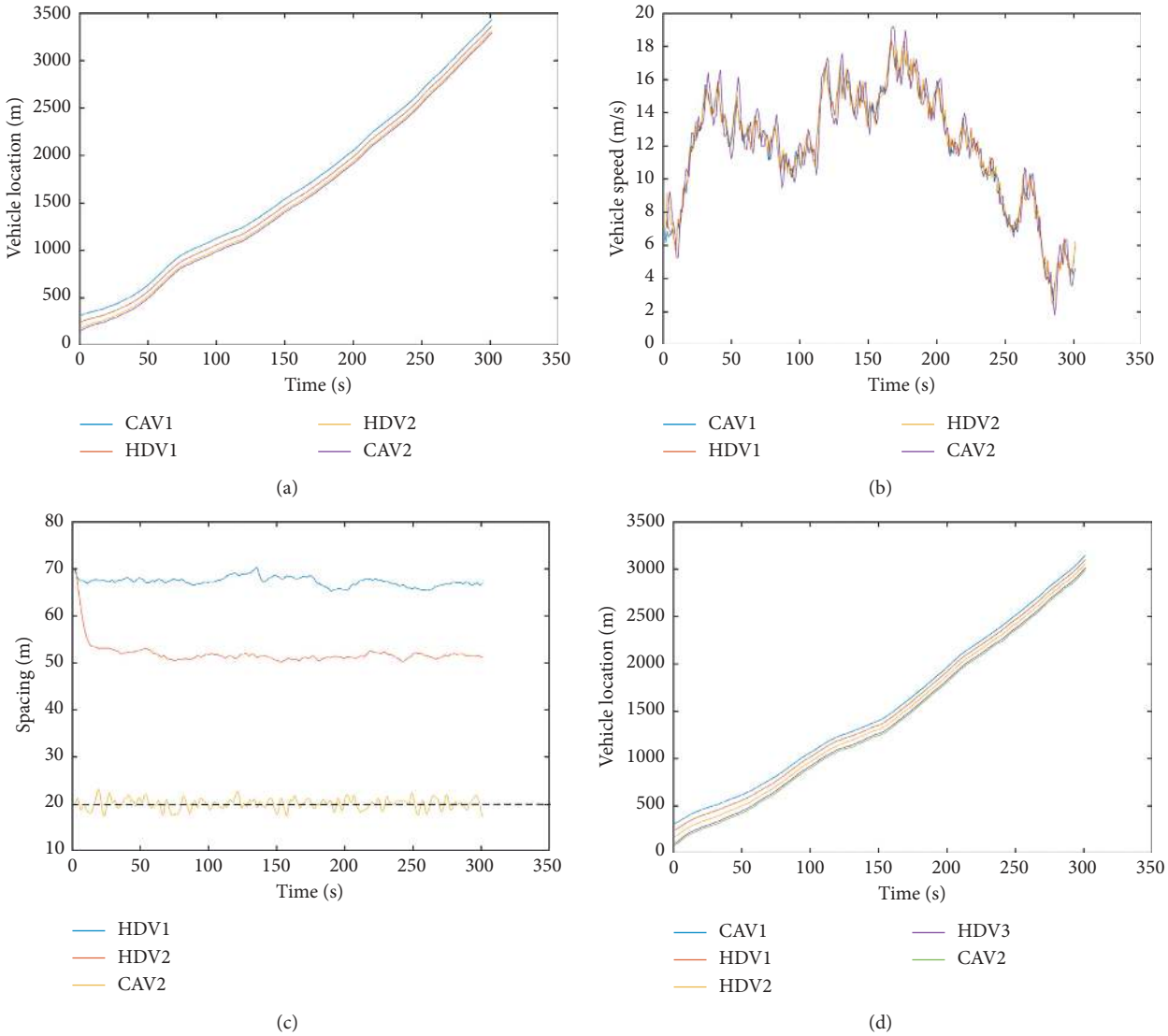

Figure 11: Continued.

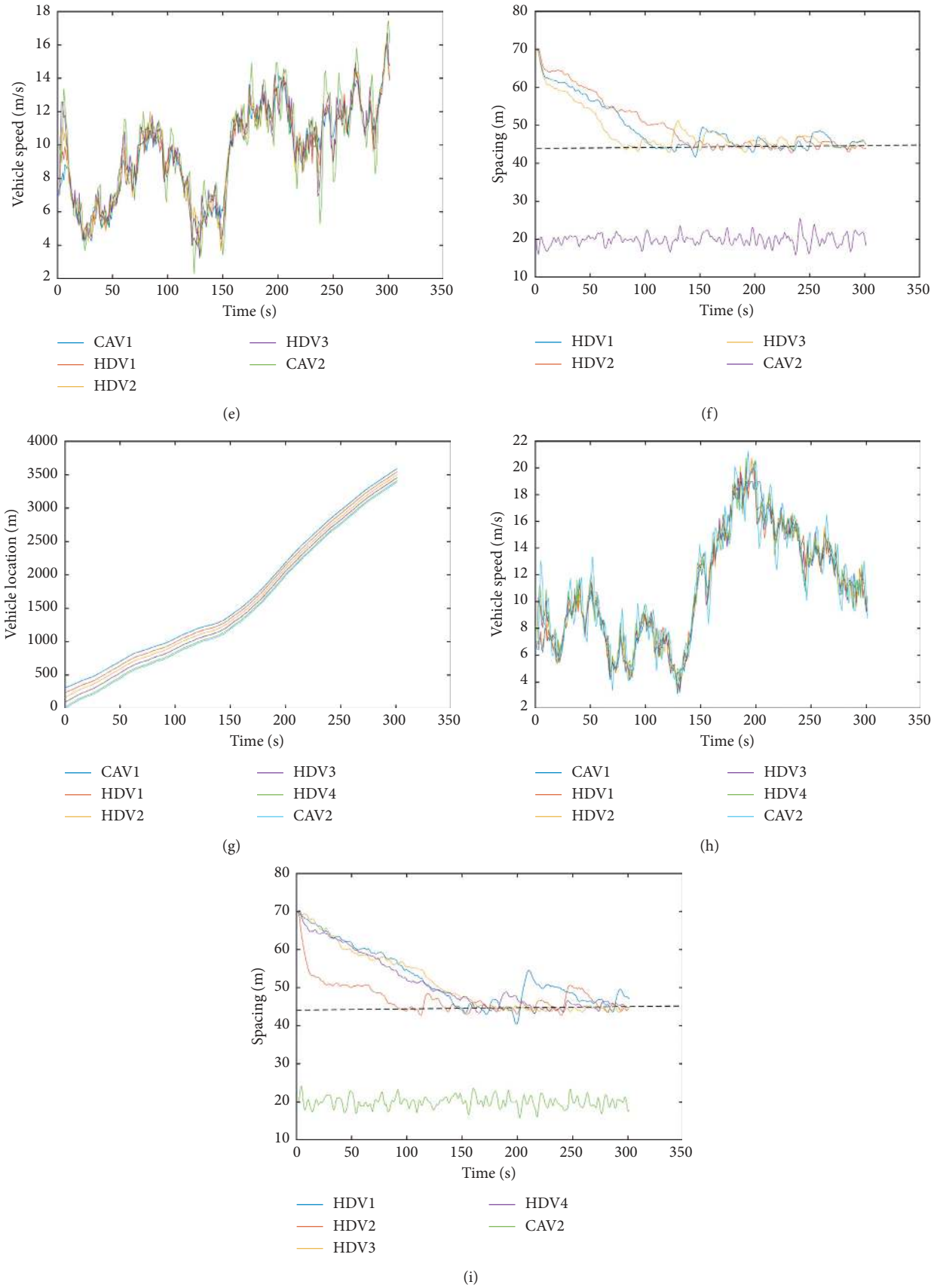

Figure 11: The driving situations of the fleet in change 1, change 2, and change 3. (a) The vehicle location of CAVs and HDVs (change 1). (b) The vehicle speed of CAVs and HDVs (change 1). (c) The spacing of formation (change 1). (d) The vehicle location of CAVs and HDVs (change 2). (e) The vehicle speed of CAVs and HDVs (change 2). (f) The spacing of formation (change 2). (g) The vehicle location of CAVs and HDVs (change 3). (h) The vehicle speed of CAVs and HDVs (change 3). (i) The spacing of formation (change 3).

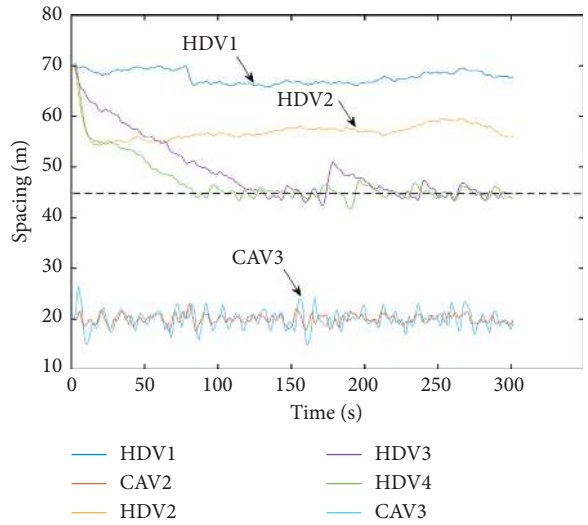

Figure 12: The spacing of formation (change 4).

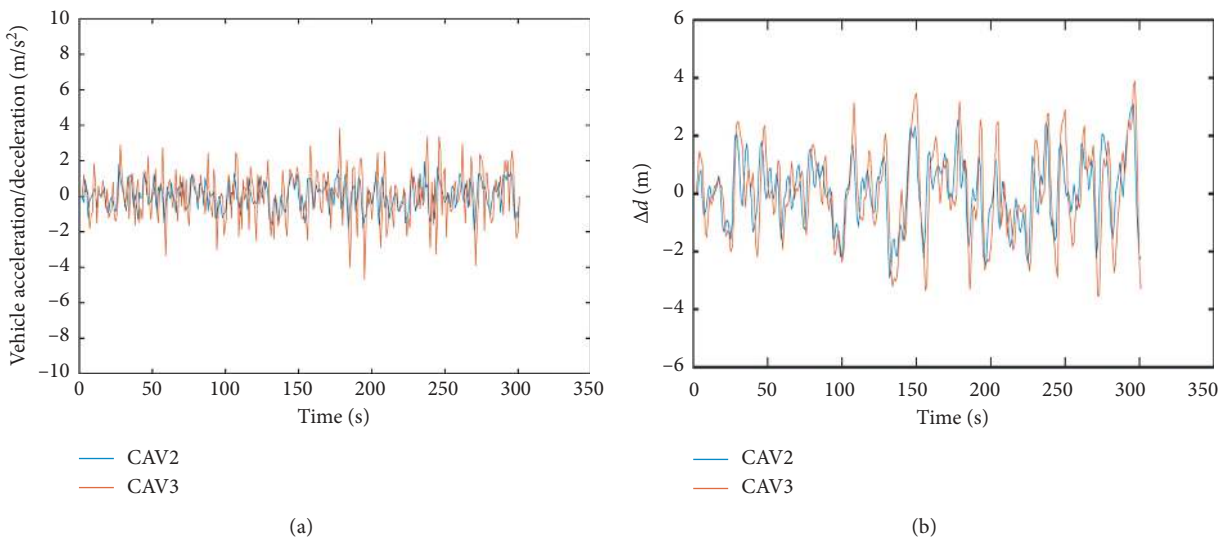

Figure 13: The fleet control under low stability requirement. (a) The acceleration of CAVs. (b) The control error of CAVs.

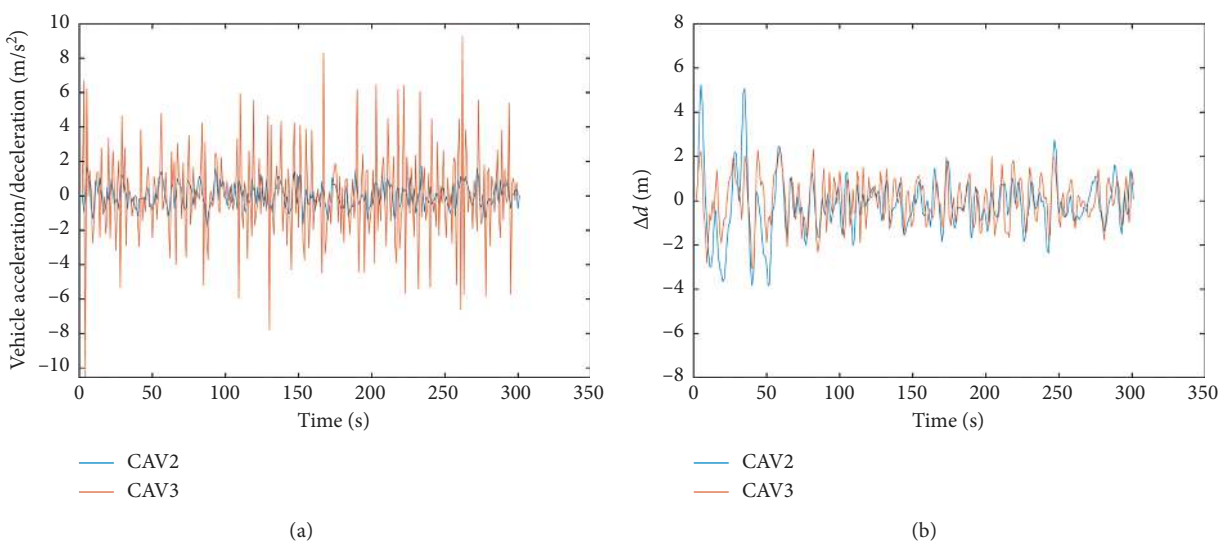

Figure 14: The fleet control under high stability requirement. (a) The acceleration of CAVs. (b) The control error of CAVs.

corresponding parameters are set as in Table 2. The experiments are checked under the low control quality and high control quality for the fleet in dense fog environment, respectively. The experiments results are shown in Figures 13 and 14.

As shown in Figure 13(a), CAV(3) and CAV(2) are not significantly difference in acceleration. However, the control error of CAV(3) is greater than the CAV(2), as shown in Figure 13(b). In Figure 14(a), CAV(3) is greater than the CAV(2) in acceleration, but the control error of CAV(3) is smaller than the CAV(2), as shown in Figure 14(b). The reason is that when the fleet is controlled under low stability requirements, the system has low control requirements for the CAV(3). CAV(3) performs the control strategy without pursuing the purpose of reducing errors in the fleet. In this situation, due to the randomness of HDV, the control error of CAV(3) will be greater than that of the CAV(2). However, when the fleet is controlled under high stability requirement, the CAV(3) must ensure the control error is smaller than the CAV(2). As to achieve this requirement and offset the randomness of HDVs, the CAV(3) needs to perform larger acceleration or deceleration. It can be concluded that the string stability of fleet is not easy to pursue. However, it is feasible to seek the balance of control efficiency and stability in fleet control based on DMPC by using a reasonable acceleration range for CAVs to make the fleet safety in passing through the dense fog environment.

5. Conclusions

This paper provides a control model for the fleet mixed with HDVs and CAVs in dense fog environment on highway based on distributed model prediction control (DMPC). Firstly, the state space model of CAVs is proposed to describe the state of CAVs within the fleet in dense fog environment. The paper used the discretization equation to describe the dynamical changing of state of CAVs in the fleet control. Secondly, a car-following model of HDVs in dense fog environment on highway is presented. It is used to describe the characteristic of the driver in dense fog environment as to follow the AGV within the scope of visibility and keep safety distance from the AGV. The simulation results show that the phenomenon shown in the simulation is consistent with the assumptions of HDV driver characteristics and fall into the relationship of speed and visibility as studied by Siebert and Wallis [45]. Thirdly, the distributed serial model predictive control (DMPC) model is used to control the fleet in dense fog environment. The controlling procedure is divided into two parts: (1) the fleet state prediction and (2) the fleet control based on DMPC. Predicting the states of the system based on DMPC focuses on the HDVs perception and prediction by CAVs and transfer between CAVs. Rolling optimization based on DMPC is used to optimize the local object of fleet control in dense fog environment with constraints. Rolling implementation of the control function is used to ensure the local equilibrium state of CAVs in the fleet control. Then, the proposed fleet control model is analyzed to meet the characteristics of the system asymptotic stability, and it can provide a nonstrict string stability during passing through dense fog environment on the highway. Finally, numerical experiments under different visibility in dense fog environment on highway are used to verify the effectiveness of the proposed model. The experiments results show that the proposed DMPC control algorithm can make CAVs consistent with HDVs under different visibilities. The spacing between CAVs and HDVs can be controlled within a predetermined safety distance. The effectiveness of the DMPC-based is highly related to the penetration rates of CAVs in the fleet and the alignment of the fleet. Furthermore, the systems of the fleet controlled based on the proposed model can guarantee the local asymptotic stability and global nonstrict string stability, simultaneously.

This paper provides the approach to control the fleet mixed with HDVs and CAVs in dense fog environment on highway. However, the method and model of the present study are not free from limitations. The first limitation is that that the present study only considers the impact of visibility. However, in dense fog environment, restrictions such as road friction and driver specificity also greatly affect the fleet driving on the highway. The second limitation is that the arrangement of the fleet vehicles in this study cannot guarantee the safety of the system that the HDV follows CAV. A third limitation is that this study did not consider the effect of the delay between CAVs in DMPC control.

Furthermore, there are some topics that remain to be studied. Further research work includes the following. (1) Other restrictions, such as communication delay, road friction coefficient, and drivers' specificity in dense fog environment, should be considered in the fleet. (2) Strict string stability of the fleet can be achieved through improving CAV prediction methods or communication technology. (3) At present, only the simulator-based tests are performed; the hardware experiments, in-vehicle tests, and scenarios' tests for the proposed modeling methods should be carried out in the future.

Data Availability

The data used to support the findings of this study are available from the corresponding author upon request.

Conflicts of Interest

The authors declare that there are no conflicts of interest regarding the publication of this paper.

Acknowledgments

The authors acknowledge the National Natural Science Foundation of China (Grant nos. 51408257 and 51308248), the Youth Scientific Research Fund of Jilin (Grant no. 20180520075JH), and the Science and Technology Project of Jilin Provincial Education Department (Grant nos. JJKH20170810KJ and JJKH20180150KJ) that partly support this work.

References

[1] A. Alim, A. Joshi, F. Chen, and C. T. Lawson, "Techniques for efficient detection of rapid weather changes and analysis of their impacts on a highway network," *Geoinformatica*, vol. 24, p. 31, 2020.

[2] C. Li, *"Research on expressway traffic flow characteristics, traffic guidance and control under adverse weather,"* Beijing University of Technology, Beijing, China, Ph.D. Dissertation, 2015.

[3] Z. Lu, T. J. Kwon, and L. Fu, "Effects of winter weather on traffic operations and optimization of signalized intersections," *Journal of Traffic and Transportation Engineering (English Edition)*, vol. 6, no. 2, pp. 196–208, 2019.

[4] C. Xu, W. Wang, and P. Liu, "Identifying crash-prone traffic conditions under different weather on freeways," *Journal of Safety Research*, vol. 46, pp. 135–144, 2013.

[5] C. Chen, X. Zhao, H. Liu, G. Ren, and X. Liu, "Influence of adverse weather on drivers' perceived risk during car following based on driving simulations," *Journal of Modern Transportation*, vol. 27, no. 4, pp. 282–292, 2019.

[6] J. O. Brooks, M. C. Crisler, N. Klein et al., "Speed choice and driving performance in simulated foggy conditions," *Accident Analysis & Prevention*, vol. 43, no. 3, pp. 698–705, 2011.

[7] Z. Xuguang and G. Jianping, "Research on the fixation transition behavior of drivers on expressway in foggy environment," *Safety Science*, vol. 119, pp. 70–75, 2019.

[8] M. M. Ahmed, M. Abdel-Aty, J. Lee, and R. Yu, "Real-time assessment of fog-related crashes using airport weather data: a feasibility analysis," *Accident Analysis & Prevention*, vol. 72, pp. 309–317, 2014.

[9] Y. Wang, L. Liang, and L. Evans, "Fatal crashes involving large numbers of vehicles and weather," *Journal of Safety Research*, vol. 63, pp. 1–7, 2017.

[10] Q. Q. Shangguan, T. Fu, and S. Liu, "Investigating rear-end collision avoidance behavior under varied foggy weather conditions: a study using advanced driving simulator and survival analysis," *Accident Analysis and Prevention*, vol. 139, p. 14, Article ID 105499, 2020.

[11] J.-h. Tan, "Impact of risk illusions on traffic flow in fog weather," *Physica A: Statistical Mechanics and Its Applications*, vol. 525, pp. 216–222, 2019.

[12] F. Rosey, I. Aillerie, S. Espie, and F. Vienne, "Driver behaviour in fog is not only a question of degraded visibility-a simulator study," *Safety Science*, vol. 95, pp. 50–61, 2017.

[13] Y. Wu, M. Abdel-Aty, J. Park, and R. M. Selby, "Effects of real-time warning systems on driving under fog conditions using an empirically supported speed choice modeling framework," *Transportation Research Part C: Emerging Technologies*, vol. 86, pp. 97–110, 2018.

[14] B. Zhai, J. Lu, Y. Wang, and B. Wu, "Real-time prediction of crash risk on freeways under fog conditions," *International Journal of Transportation Science and Technology*, 2020, In press.

[15] H. M. Hassan and M. A. Abdel-Aty, "Predicting reduced visibility related crashes on freeways using real-time traffic flow data," *Journal of Safety Research*, vol. 45, pp. 29–36, 2013.

[16] T. Winkle, C. Erbsmehl, and K. Bengler, "Area-wide real-world test scenarios of poor visibility for safe development of automated vehicles," *European Transport Research Review*, vol. 10, no. 2, p. 15, 2018.

[17] Y. Wu, M. Abdel-Aty, J. Park, and J. Zhu, "Effects of crash warning systems on rear-end crash avoidance behavior under fog conditions," *Transportation Research Part C: Emerging Technologies*, vol. 95, pp. 481–492, 2018.

[18] Z. Li, Y. Li, P. Liu, W. Wang, and C. Xu, "Development of a variable speed limit strategy to reduce secondary collision risks during inclement weathers," *Accident Analysis & Prevention*, vol. 72, pp. 134–145, 2014.

[19] D. Chen, A. Srivastava, S. Ahn, and T. Li, "Traffic dynamics under speed disturbance in mixed traffic with automated and non-automated vehicles," *Transportation Research Part C: Emerging Technologies*, vol. 113, pp. 293–313, 2020.

[20] S. Bahrami and M. J. Roorda, "Optimal traffic management policies for mixed human and automated traffic flows," *Transportation Research Part A: Policy and Practice*, vol. 135, pp. 130–143, 2020.

[21] G. Munster and A. Bohlig, "Auto outlook 2040: the rise of fully autonomous vehicles," 2020, https://loupventures.com/auto-outlook-2040-the-rise-of-fully-autonomous-vehicles.

[22] Ministry of Sicence and Technology of the People's Republic of China, *"Research And Development Guideline- Comprehensive Transportation And Intelligent Transportation,"* Ministry of Sicence and Technology of the People's Republic of China, Beijing, China, 2020, http://www.most.gov.cn/.

[23] C. Jianyang, "Dense fog and freeway traffic accidents," *Journal of Highway and Transportation Research and Development*, vol. 15, no. 2, pp. 38–40, 1998.

[24] W. Wang, Q. Cheng, C. Li, D. André, and X. Jiang, "A cross-cultural analysis of driving behavior under critical situations: a driving simulator study," *Transportation Research Part F: Traffic Psychology and Behaviour*, vol. 62, pp. 483–493, 2019.

[25] R. Mu and T. Yamamoto, "An analysis on mixed traffic flow of conventional passenger cars and microcars using a cellular automata model," *Procedia-Social and Behavioral Sciences*, vol. 43, pp. 457–465, 2012.

[26] G. H. Bham and R. F. Benekohal, "A high fidelity traffic simulation model based on cellular automata and car-following concepts," *Transportation Research Part C: Emerging Technologies*, vol. 12, no. 1, pp. 1–32, 2004.

[27] L. Yang, J. Zheng, Y. Cheng, and B. Ran, "An asymmetric cellular automata model for heterogeneous traffic flow on freeways with a climbing lane," *Physica A: Statistical Mechanics and Its Applications*, vol. 535, Article ID 122277, 2019.

[28] S. Maerivoet and B. De Moor, "Cellular automata models of road traffic," *Physics Reports*, vol. 419, no. 1, pp. 1–64, 2005.

[29] S. Gong and L. Du, "Cooperative platoon control for a mixed traffic flow including human drive vehicles and connected and autonomous vehicles," *Transportation Research Part B: Methodological*, vol. 116, pp. 25–61, 2018.

[30] Y. Zhou, M. Wang, and S. Ahn, "Distributed model predictive control approach for cooperative car-following with guaranteed local and string stability," *Transportation Research Part B: Methodological*, vol. 128, pp. 69–86, 2019.

[31] S. Gong, J. Shen, and L. Du, "Constrained optimization and distributed computation based car following control of a connected and autonomous vehicle platoon," *Transportation Research Part B: Methodological*, vol. 94, pp. 314–334, 2016.

[32] Y. Wu, M. Abdel-Aty, Q. Cai, J. Lee, and J. Park, "Developing an algorithm to assess the rear-end collision risk under fog conditions using real-time data," *Transportation Research Part C: Emerging Technologies*, vol. 87, pp. 11–25, 2018.

[33] X. Yu, "Study of zero-order holder discretization in single input sliding mode control systems," in *Proceedings of the IEEE International Symposium on Circuits & Systems*, Florence, Italy, 2008.

[34] S. Barnett, "Linear system theory and design," *Automatica*, vol. 22, no. 3, pp. 385-386, 1986.

[35] F. Rosey, I. Aillerie, S. Espié, and F. Vienne, "Driver behaviour in fog is not only a question of degraded visibility - a simulator study," *Safety Science*, vol. 95, pp. 50–61, 2017.

[36] K. Gao, H. Tu, H. Shi, and Z. Li, "Effects of low visibility in haze weather on driving behaviors in different car following states," *Journal of Jilin University (Engineering Edition)*, vol. 47, no. 6, pp. 1717–1727, 2017.

[37] A. Hegyi, B. De Schutter, and H. Hellendoorn, "Model predictive control for optimal coordination of ramp metering and variable speed limits," *Transportation Research Part C: Emerging Technologies*, vol. 13, no. 3, pp. 185–209, 2005.

[38] W. B. Dunbar and R. M. Murray, "Distributed receding horizon control for multi-vehicle formation stabilization," *Automatica*, vol. 42, no. 4, pp. 549–558, 2006.

[39] J. Ploeg, E. Semsar-Kazerooni, G. Lijster, N. van de Wouw, and H. Nijmeijer, "Graceful degradation of cooperative adaptive cruise control," *IEEE Transactions on Intelligent Transportation Systems*, vol. 16, no. 1, pp. 488–497, 2015.

[40] D. Chen, J. Laval, Z. Zheng, and S. Ahn, "A behavioral car-following model that captures traffic oscillations," *Transportation Research Part B: Methodological*, vol. 46, no. 6, pp. 744–761, 2012.

[41] S. V. Rakovic, E. C. Kerrigan, K. I. Kouramas, and D. Q. Mayne, "Invariant approximations of the minimal robust positively Invariant set," *IEEE Transactions on Automatic Control*, vol. 50, no. 3, pp. 406–410, 2005.

[42] Z. Sun and S. S. Ge, *Stability Theory of Switched Dynamical Systems (Communications and Control Engineering)*, Springer-Verlag, London, UK, 2011.

[43] A. Bacciotti and L. Rosier, *Lyapunov Functions and Stability in Control Theory (Communications and Control Engineering)*, Springer-Verlag, Berlin, Germany, 2005.

[44] D. Q. Mayne, J. B. Rawlings, C. V. Rao, and P. O. M. Scokaert, "Constrained model predictive control: stability and optimality," *Automatica*, vol. 36, no. 6, pp. 789–814, 2000.

[45] F. W. Siebert and F. L. Wallis, "How speed and visibility influence preferred headway distances in highly automated driving," *Transportation Research Part F: Traffic Psychology and Behaviour*, vol. 64, pp. 485–494, 2019.